

Synaptosomes: New Vesicles for Neuronal Mitochondrial Transplantation

Pasquale Picone

National Research Council: Consiglio Nazionale delle Ricerche

Gaetana Porcelli

National Research Council: Consiglio Nazionale delle Ricerche

Celeste Caruso Bavisotto

University of Palermo: Universita degli Studi di Palermo

Domenico Nuzzo

National Research Council: Consiglio Nazionale delle Ricerche

Giacoma Galizzi

National Research Council: Consiglio Nazionale delle Ricerche

Pier Luigi San Biagio

National Research Council: Consiglio Nazionale delle Ricerche

Donatella Bulone

National Research Council: Consiglio Nazionale delle Ricerche

Marta Di Carlo (✉ marta.dicarlo@irib.cnr.it)

National Research Council: Consiglio Nazionale delle Ricerche <https://orcid.org/0000-0002-7934-1275>

Research

Keywords: synaptosomes, mitochondria, neurodegeneration, delivery system, mitochondrial transplantation

Posted Date: October 15th, 2020

DOI: <https://doi.org/10.21203/rs.3.rs-89848/v1>

License:   This work is licensed under a Creative Commons Attribution 4.0 International License.

[Read Full License](#)

Version of Record: A version of this preprint was published on January 6th, 2021. See the published version at <https://doi.org/10.1186/s12951-020-00748-6>.

Synaptosomes: new vesicles for neuronal mitochondrial transplantation

Pasquale Picone¹, Gaetana Porcelli¹, Celeste Caruso Bavisotto^{2,3,4}, Domenico Nuzzo¹, Giacomina Galizzi¹, Pier Luigi San Biagio², Donatella Bulone², Marta Di Carlo^{1*}

1. Istituto per la ricerca ed Innovazione Biomedica (IRIB) CNR via U. La Malfa 153, 90146, Palermo, Italy

2. Istituto di Biofisica (IBF) (sez. Palermo) CNR, via U. La Malfa, 153, I-90146 Palermo, Italy

3. Dipartimento di Biomedicina, Neuroscienze, e Diagnostica Avanzata (BIND) (sez. Anatomia Umana)
Università di Palermo, via del Vespro 129, 90127 Palermo, Italy

4. Istituto Euro-Mediterraneo di Scienze e Tecnologie (IEMEST), via M. Miraglia, 20, 90139 Palermo, Italy

*Correspondence Marta Di Carlo IRIB-CNR, Palermo, Italy

e-mail: marta.dicarlo@irib.cnr.it

Abstract

Background: Mitochondrial dysfunction is a critical factor in the onset and progression of neurodegenerative diseases. Recently, mitochondrial transplantation has been advised as an innovative and attractive strategy to transfer and replace damaged mitochondria. Here we propose, for the first time, to use rat brain extracted synaptosomes, subcellular fraction of isolated synaptic terminal that contain mitochondria, as mitochondrial delivery systems.

Results: Synaptosomes preparation was validated by the presence of Synaptophysin and PSD95. Synaptosomes were characterized in terms of dimension, zeta potential, polydispersity index and number of particles/mL. Nile Red or CTX-FITC labeled synaptosomes were internalized in LAN5 recipient cells by a mechanism involving specific protein-protein interaction, as demonstrated by loss of fusion ability after trypsin treatment and using different cell lines. The loading and release ability of the synaptosomes was proved by the presence of curcumin both into synaptosomes and LAN5 cells. The vitality of mitochondria transferred by Synaptosomes was demonstrated by the presence of Opa1, Fis1 and TOM40 mitochondrial proteins and JC-1 measurements. Further, synaptosomes deliver vital mitochondria into the cytoplasm of neuronal cells as demonstrated by microscopic images, increase of TOM 40, cytochrome c, Hexokinase II mitochondrial proteins, and presence of rat mitochondrial DNA. Finally, by using synaptosomes as vehicle, healthy mitochondria restored mitochondrial function in cells containing rotenone or CCCp damaged mitochondria.

Conclusions: Taken together these results suggest that synaptosomes can be a natural vehicle for the delivery of molecules and organelles to neuronal cells. Further, replacement of affected mitochondria with healthy ones could be a potential therapy for the treatment of neuronal mitochondrial dysfunction-related diseases.

Keywords: synaptosomes; mitochondria; neurodegeneration; delivery system; mitochondrial transplantation;

Background

Neurodegenerative diseases (NDs) are age-related debilitating disorders characterized by progressive loss of structural and functional neurons. It has been estimated that approximately 30 million people worldwide are affected by NDs and the number is expected to exceed 150 million in 2050 [1]. The lack of any effective treatment makes these pathologies a major public health. NDs, including Alzheimer's disease (AD), Parkinson's disease (PD), and Huntington's disease (HD), are characterized by accumulation of aggregates of misfolded proteins in specific areas of the brain [1]. These pathologies are known to be multifactorial disorders, but one of the most accepted assumptions is that mitochondrial dysfunction is a critical factor in their onset and progression [1-4]. Mitochondria are the main source of energy metabolism and play a relevant role in several cell functions such as calcium homeostasis, reactive oxygen species (ROS) production, cell survival and proliferation, control of apoptosis and autophagy [3]. Mitochondria are dynamic organelles capable of changing size, shape and position according to the physiological needs of the cells. They move along microtubules within the cell providing the energy for the different functions including those relating to synapses. Mitochondrion wellness is crucial for cellular homeostasis and its impairment is linked to several neurodegenerative diseases. Mitochondrial dysfunction is associated with altered antioxidant defence or excessive ROS generation. The use of natural antioxidants molecules with medicinal value as potential therapy for the prevention and treatment of NDs has been largely explored [4,5]. Antioxidant such as resveratrol, green tea polyphenol, epigallocatechin gallate (EGCG) or ferulic acid were found to exert beneficial effects both *in vitro* or *in vivo* models of AD and other neurodegenerative diseases [6-9]. Although quite controversial, some studies in humans report that the administration of high-dose combined vitamin E and vitamin C is associated with a slowed progression of PD. Further, the beneficial effect can be improved by encapsulating the antioxidant molecules into nanoparticles capable of enhancing drug transport through the Blood Brain Barrier (BBB) [10, 11]. Studies *in vitro* have reported that insulin, acting as antioxidant molecule, is able to prevent mitochondrial oxidative stress and apoptosis by inhibiting the PI3K/AKT cell survival signaling pathway [12, 13]. Recent evidence has demonstrated that insulin delivery to the brain can be an effective pharmacological therapy for some neurodegenerative pathologies and the intranasal route of administration furtherly increases the efficacy and safety of the treatment [14]. However, all these strategies to contrast mitochondrial stress cannot be considered as an effective prevention or therapy for NDs and the possibility to replace damaged mitochondria result be extremely attractive. Mitochondria have a life cycle in which mitochondrial dynamics and mitophagy contribute to quality control. Dynamics of mitochondria is regulated by fusion and fission events. These mechanisms

are controlled by specific proteins such as mitofusin 1 (MNF1) and optic atrophy protein1 (OPA1) for fusion, and dynamin related protein-1 (Drp1) and fission1 (FIS1) for fission.¹⁵ When mitochondria are damaged, the organelles can be recovered by fusing with healthy mitochondria or eliminated by mitophagy. However, when damaged mitochondria cannot be replaced or restored, the possibility to transfer healthy mitochondria from one cell to another represents an attractive therapeutic strategy. With the name of mitochondrial transplantation is now indicated the transfer of alive mitochondria into injured cells for the treatment of different diseases, including NDs [16-19].

Some strategies such as direct microinjection of isolated mitochondria, cell-mediated transfer utilizing tunneling nanotubes, vesicle- or liposomes-mediated delivery, and systemic delivery have been employed to permit mitochondria uptake and increase transplantation efficiency [19]. Nevertheless, adverse effect such as inflammatory or immune response or introduction of cellular element in addition to mitochondria can interfere with the transplantation efficacy [19]. Recently, an increased incorporation efficiency was observed when isolated mitochondria from a healthy individual were conjugated with the carrier peptide Pep-1 [20]. However, delivery approaches have to be optimized on the basis of the tissue or cell type.

Synaptosomes are a subcellular fraction of isolated synaptic terminal prepared by homogenization and gradient centrifugation of brain tissue. The term “synaptosome” was coined by Whittaker (1964)²¹ who studied the localization of neurotransmitters and the functional components of the synapses. Synaptosomes contain numerous synaptic vesicles and mitochondria are considered a relevant model system for studying human synaptic dysfunction in NDs [22]. Although the use of cells or cell membrane-based drug delivery systems has been investigated [23, 24] the possibility of using a subcellular structure for organelle delivery has never been studied. Here, for the first time, we propose to use a synaptosome-based mitochondria delivery system to transfer healthy mitochondria to neuronal target cells. Furthermore, the possibility to replace CCCp- or rotenone-damaged mitochondria by transplantation of healthy mitochondria vehiculated by synaptosomes in neuronal cells was evaluated.

Results

Isolation and characterization of rat synaptosomes

Synaptosomes, extracted from the pre- and post-synaptic components (Fig. 1 A), were isolated by sucrose density gradient ultracentrifugation of the fresh rat brain homogenate. The presence of synaptosomes in the collected band (Fig. 1 B) was ascertained by detecting with Western blot experiments the presence of two specific pre-synaptic and post-synaptic markers, Synaptophysin and PSD95 respectively (Fig. 1 C). A major content of these two proteins was found in the collected band with respect to the total homogenate (Fig. 1 C and D) so confirming the success of the fractionation procedure. By Dynamic Light Scattering (DLS) measurements, the size of the synaptosomes was determined to range between 0.5 and 1.5 μm with a mean diameter of about 800 microns (Fig. 1 E). AFM images (Fig. 1 F) demonstrated the typical synaptosomes features, confirming the heterogeneity of the preparation. Synaptosomal fraction was also characterized in terms of zeta potential, polydispersity index (PDI), concentration. The values are reported in Table 1.

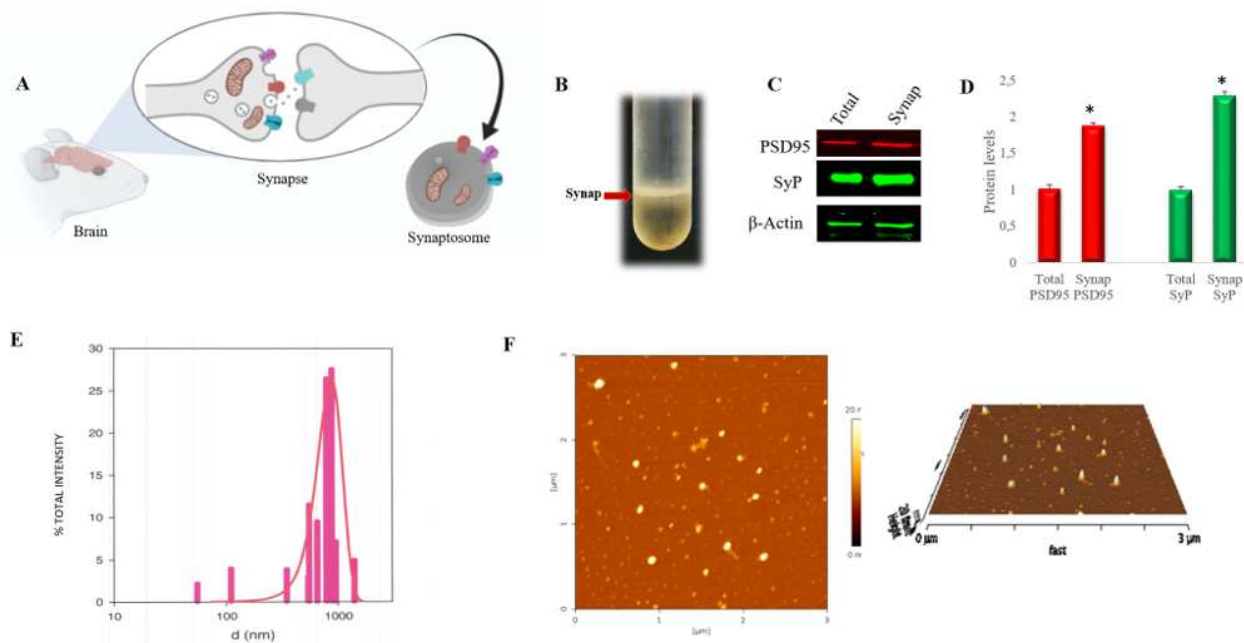


Fig. 1

Synaptosome parameters	
[Particles/mL]	5.1 x10 ⁹ ±0.7x10 ⁹
Zeta Potential [mV]	-43,5 ±
polydispersity	0.307

Table 1

Synaptosomes cell interaction and uptake

Synaptosomes are membranous sacs composed by a lipid bilayer including lipid rafts [25] and containing synaptic components. With the aim of using them as delivery systems, firstly we investigated if synaptosomes were toxic to LAN5 neuronal cells (S1). Synaptosomes were incubated with the membrane staining Nile Red (red), or with the lipid raft staining CTX (green). Results from fluorescence measurements (Fig. 2 A and B) showed that both the dyes were suitable for synaptosomes staining and therefore as vesicles tracing. To evaluate cellular uptake of synaptosomes, LAN5 cells were incubated with different amounts of synaptosomes stained with Nile Red (red) or CTX-FITC (green) and the fluorescence signal was measured (Fig. 2 C). The fluorescence intensity was observed to increase in a dose dependent manner for both the tracker dyes (Fig. 2 D and F). The interaction between synaptosomes and LAN5 was also visualized by fluorescence microscopy inspection (Fig. 2 E and G). LAN5 uptake of synaptosomes was furtherly evidenced by detecting the presence of rat synaptophysin, a presynaptic protein associated with synaptic vesicles and presynaptic membrane [26]. After administration of different amounts of synaptosomes to LAN5 cells, the presence of the rat synaptophysin was investigated (Fig. 2 H). Western blot experiments on LAN5 extracted confirmed the presence of a band of about 36 kDa corresponding to rat synaptophysin (Fig. 2, I), the band intensity was higher at larger administered doses of synaptosomes (Fig. 2 I and L), A higher band of 45 kDa with the same intensity, representing the human endogenous protein, was also observed (Fig. 2 I). As the trypsin treatment used in protein extraction, removes synaptosomes interacting with the cellular surface, it is reasonable that the detection of rat synaptophysin was due to the synaptosomes internalization or membranes fusion.

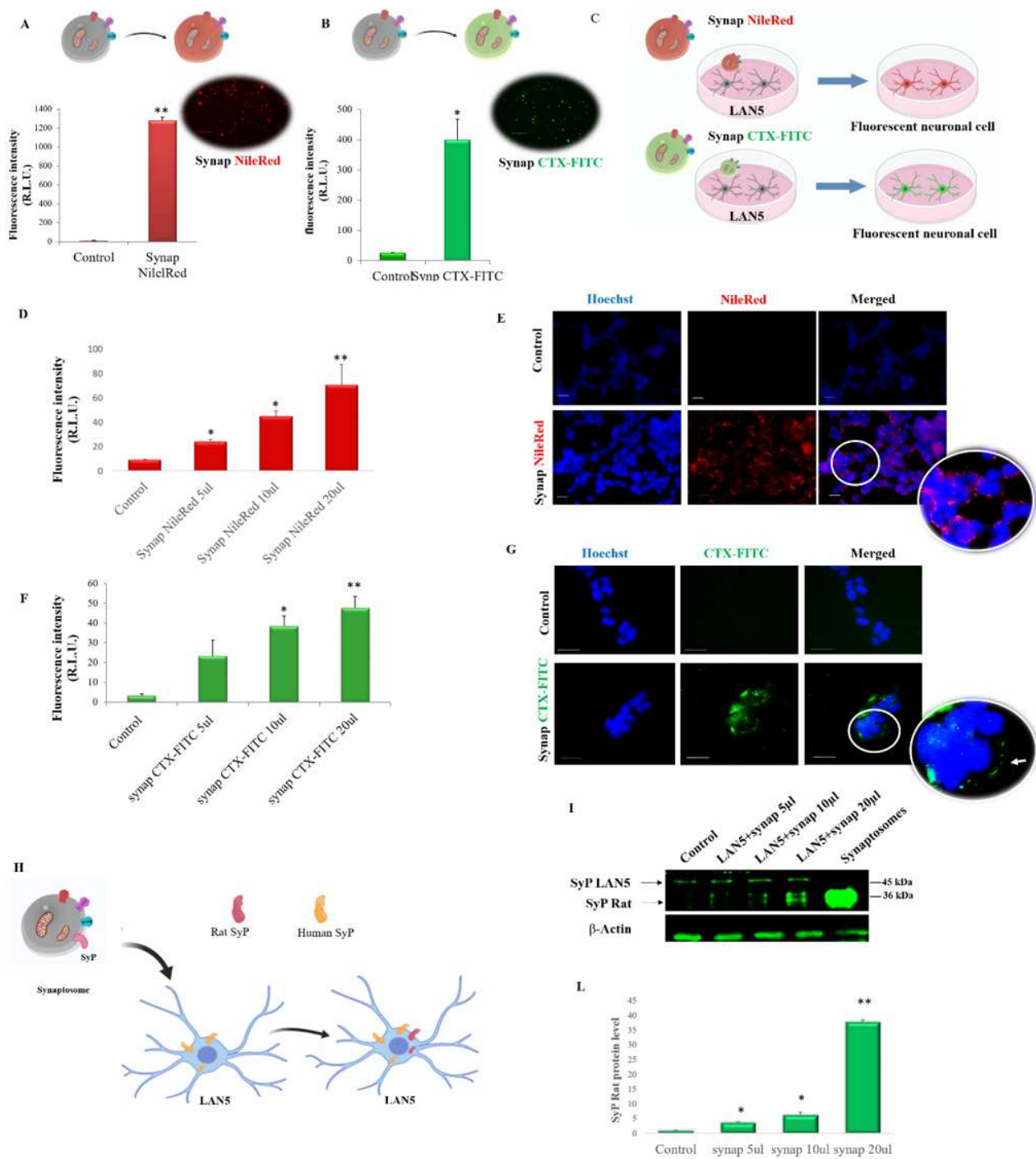


Fig. 2

Synaptosomes as potential delivery system

The ability of synaptosomes to release the cargo was tested by using curcumin, a fluorescent compound derived from the rhizome of *Curcuma longa*. It had been shown that curcumin can be loaded into lipid nanosystems and internalized in neuronal cells [27]. After curcumin addition to synaptosomes (Fig. 3 A) an increase of the fluorescence intensity was observed indicating that synaptosomes were able to incorporate curcumin. Different amounts of curcumin-loaded synaptosomes (Synap-Curcumin) were then incubated with LAN5 cells for 2 and 4 hours (Fig. 3 B). A large increase of fluorescence intensity was observed in the sample treated with 20 μ l of curcumin-loaded synaptosomes especially after 4 hours of incubation (Fig. 3 C). The results were confirmed by microscopy images (Fig. 3 D). A green fluorescence was observed in the cellular body indicating that the compound was released by the synaptosomes inside the cells (Fig. 3 D).

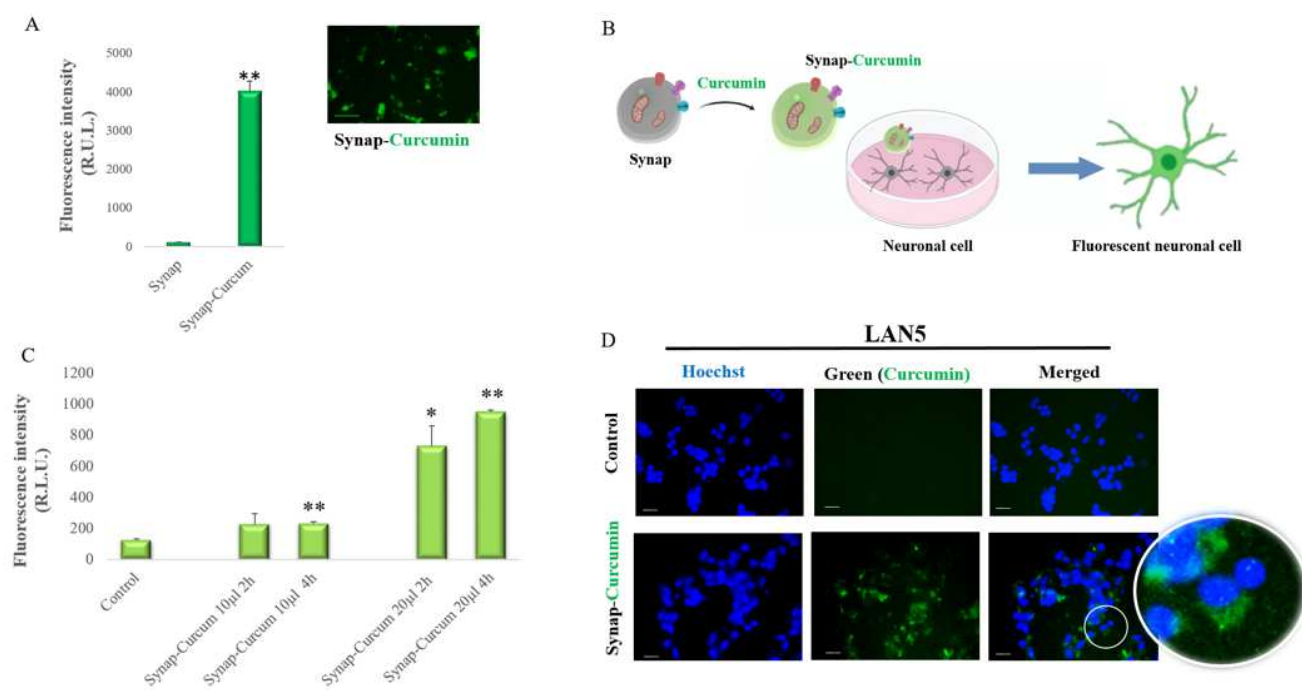


Fig. 3

Synaptosomes-specific cell interaction

To inspect whether the contact between synaptosomes and cell membrane is due to protein-protein and/or lipid-protein interaction, Nile red stained synaptosomes were treated with two different amounts of trypsin (Fig. 4 A) and incubated with LAN5 cells. The fluorescence intensity for cells incubated with synaptosomes treated with trypsin was found lower than that for cells incubated with untreated synaptosomes (Fig. 4 B). This result was confirmed by microscopic images of Fig. 4, C showing that the red signal indicating interaction between cells and synaptosomes is significantly lower in the case of trypsin treated synaptosomes. This suggests that some proteins disrupted by the trypsin treatment could play a relevant role in synaptosomes cellular uptake. Furthermore, to assess if cellular interaction and uptake of synaptosomes are neuron-specific, two amounts of Nile red stained synaptosomes were administered to different cell lines including neuronal (LAN5), epithelial (A549) and hepatic (HepG2) cells. By microscopy imaging (Fig. 4 D) and fluorescence measurements (Fig. 4 E) we observed no significant fluorescence signal for both A549 and HepG2 cells at difference with the case of LAN5 cells. This suggests that specific neuronal proteins are necessary for synaptosomes-cell interaction and uptake.

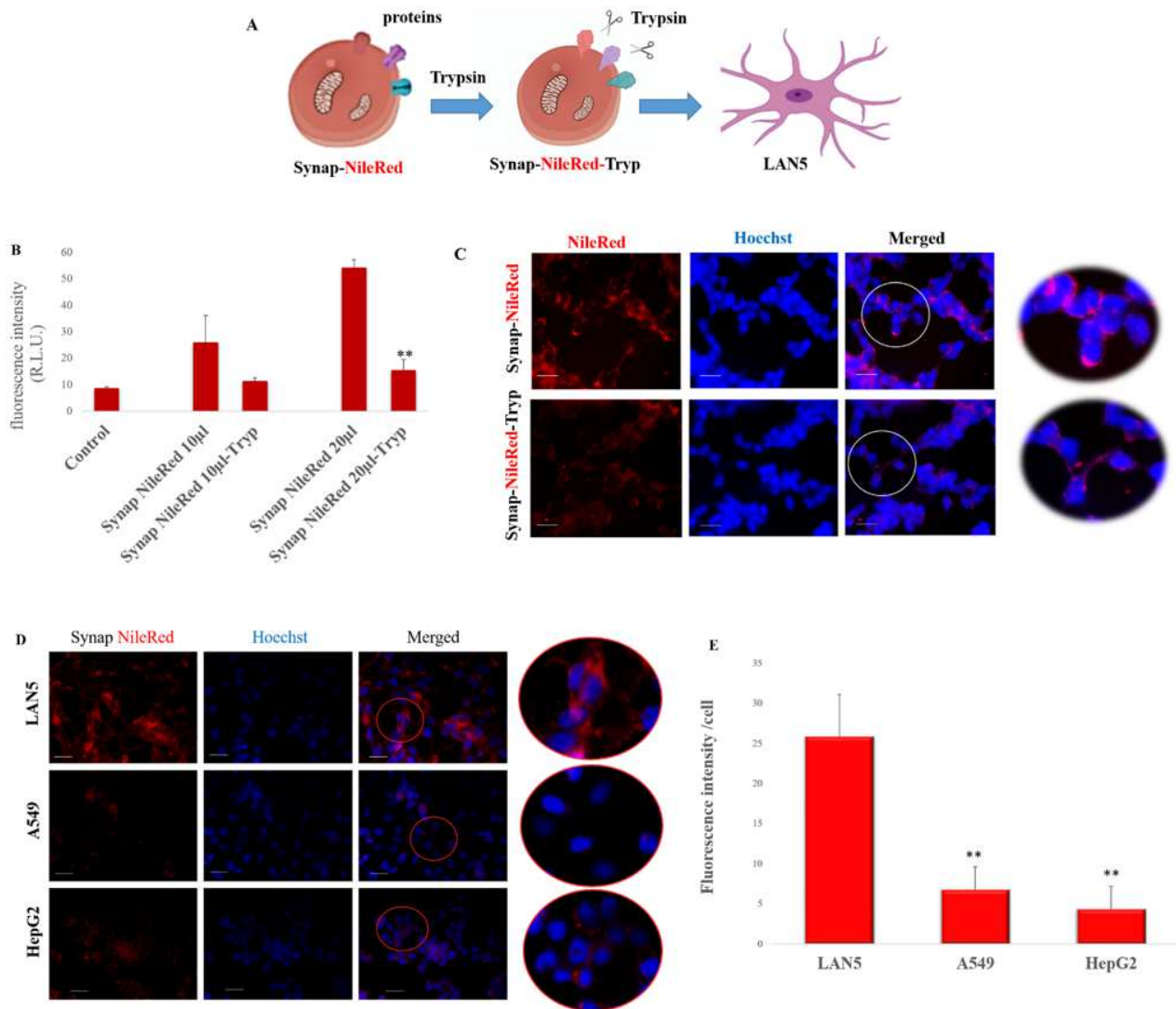


Fig. 4

Synaptosomes transport vital mitochondria that can be cryopreserved

Synaptosomes contain synaptic vesicles and often one or more mitochondria. Mitochondria presence and viability in isolated synaptosomes were analysed. The presence of mitochondrial specific proteins including the protein optic atrophy 1 (Opa1) (inner mitochondrial membrane protein), Fission 1 protein (Fis1) (outer mitochondrial membrane proteins) and Translocase of Outer Mitochondrial Membrane 40 (TOM40) in synaptosomal preparation was investigated by Western blotting analysis. All the three proteins were detected in synaptosomal fraction so indicating that synaptosomes do contain mitochondria (Fig. 5 A). This result was confirmed by staining synaptosomes with JC1, a fluorescent dye that emits red fluorescence when the mitochondrial membrane potential is high, and mitochondria are healthy (Fig. 5 B). To further validate the presence of mitochondria, synaptosomes were treated with CCCp, an inhibitor of oxidative phosphorylation. A drastic reduction of red fluorescence was observed in this case (Fig. 5 B). Representative fluorescence images for all samples are shown in Fig. 5, C. Thus, synaptosomes preparation contains functional mitochondria.

In order to test whether cryopreserved synaptosomes can be used for mitochondrial transplantation, we evaluated their physical-chemical properties and biological activity. Rat cerebral cortex synaptosomes preparation was frozen under controlled temperature steps and times (Fig. 5 D). After thawing, physical parameters such as dimensions and zeta potential were measured and compared with those of fresh synaptosomes. No significant difference was detected (Fig. 5 E). The viability of mitochondria, after freeze/thawing of synaptosomes, was assessed by JC-1 fluorescence assay. The results showed that the red and green fluorescence of the thawed synaptosomes was comparable to that of fresh synaptosomes (Fig 5 F and G), indicating that despite the temperature variations their functionality was preserved. Moreover, long-term storage of the synaptosomes up to 12 months had no influence on the valuated synaptosomal parameters (data not shown). Thus, in the next experiments, we used freeze/thawed synaptosomes.

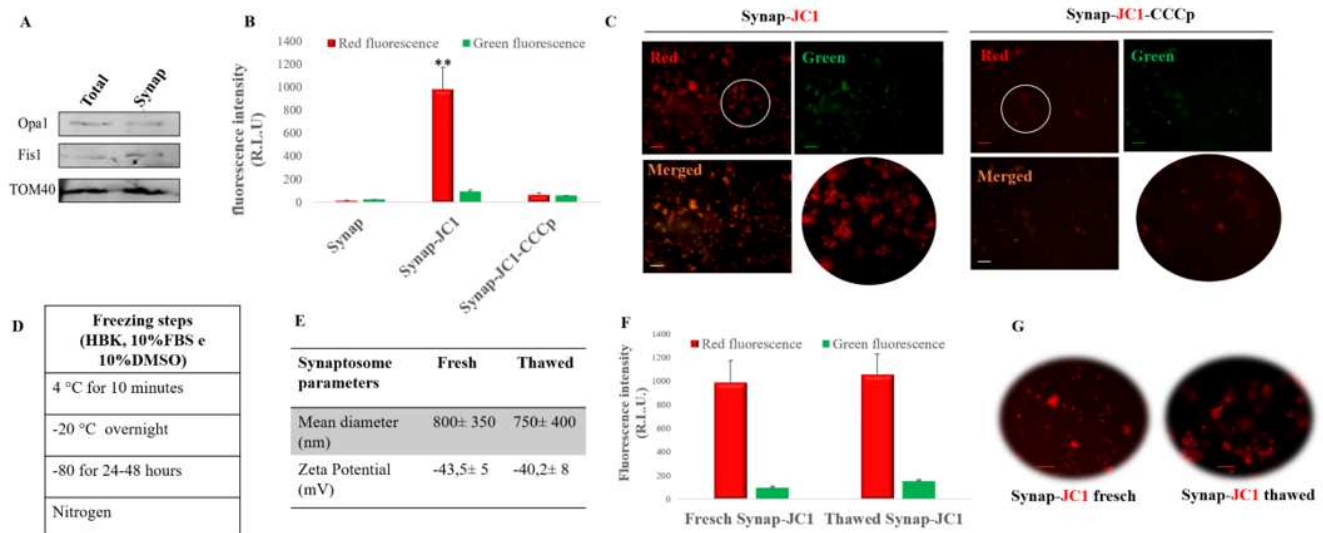


Fig. 5

Synaptosomes as mitochondrial delivery systems

We explored the possibility to use synaptosomes to transfer functional mitochondria in cell. There are various techniques for mitochondrial transplantation, but the possibility to use synaptosomes as delivery system has not yet been explored. To test this possibility, synaptosomes containing JC1 stained mitochondria (Synap-JC1) were administrated to LAN5 cells and incubated for two different time intervals (Fig. 6 A). After two hours of incubation, a light punctate red fluorescence was detected by fluorescence microscopy on LAN5 membranes, whereas after 4 hours an intense red fluorescence was observed in LAN5 cytoplasm indicating that cellular uptake of the synaptosomal-mitochondria was occurred (Fig. 6 B). Dynamic imaging simulation was performed to fully detect uptake and trafficking of Synap-JC-1. As shown in Fig. 6 C, after 2 hours some synaptosomes were approaching the cells while others were interacting with the cellular membrane. After 4 hours, Synapt-JC-1 were absorbed by the cells. The increase in mitochondrial uptake over time was confirmed by fluorescence measurements that showed a major fluorescence intensity inside the cells after 4 hours (Fig. 6 D). The efficiency of mitochondrial cell delivery, defined as the percentage of live cells receiving mitochondria, was around 40% after 4 hours.

As a further check, the presence of specific mitochondrial proteins such as TOM40, Cytochrome c and Hexokinase II was searched in recipient cells after incubation with their specific antibodies. Fig. 6 E and F shows that the amount of all three proteins is much larger than in control. Finally, to confirm the occurrence of mitochondrial transfer, PCR analysis was performed. As expected, the amount of Rat

mtDNA (mitochondrial DNA) significantly increased in LAN5 cells proportionally to the amount of synaptosomes administrated, whereas Human mtDNA and nDNA (nuclear DNA) did not change, (Fig.6 G). Thus, synaptosomes can be considered a valid delivery system for transplanting healthy mitochondria.

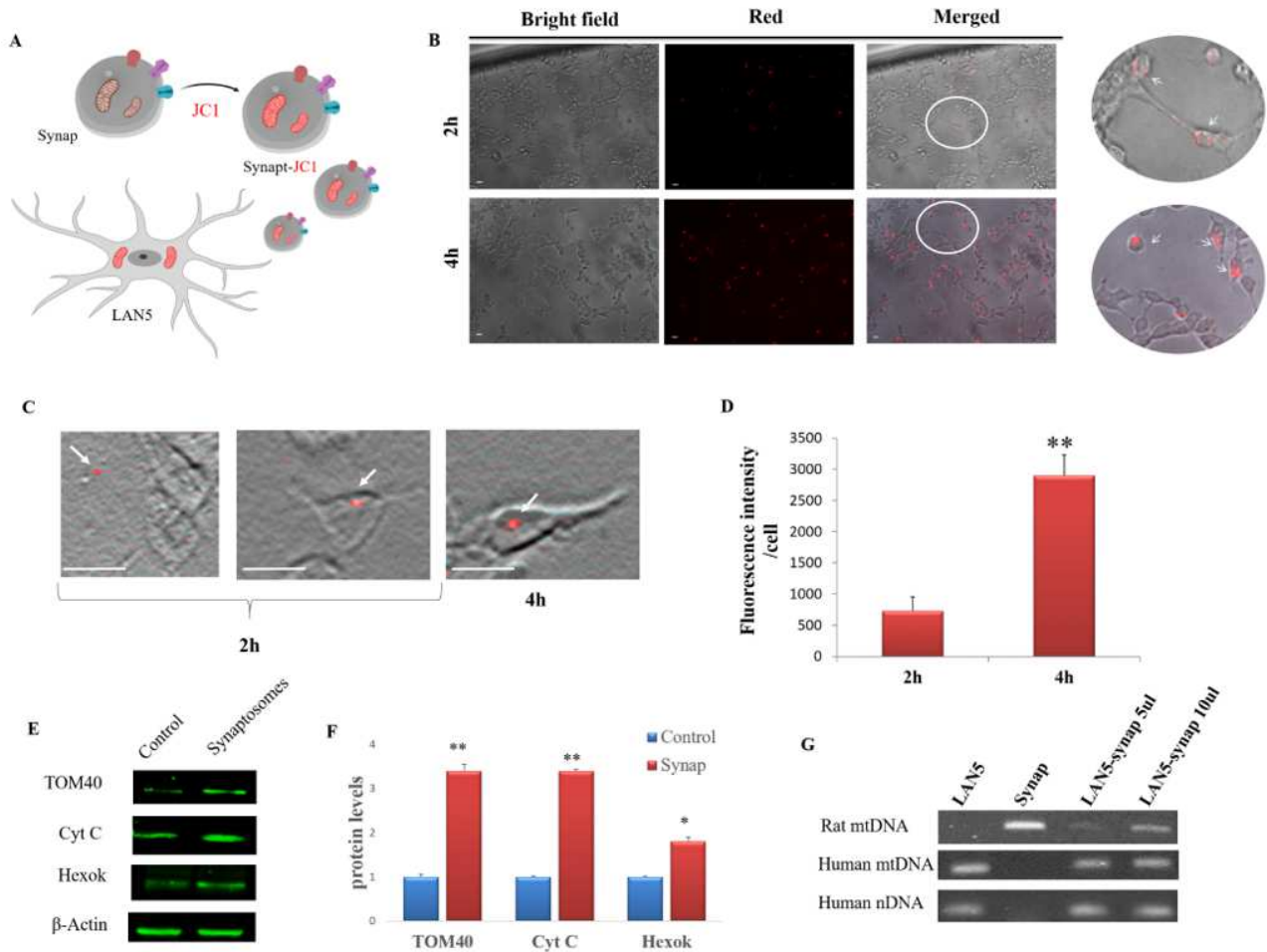


Fig. 6

Restore of mitochondrial homeostasis by mitochondrial transfer

We investigated the possibility to replace damaged with healthy mitochondria within a cell by using synaptosomes as vehicle. To this purpose, we treated LAN5 cells with CCCp or Rotenone, two compounds that induce mitochondrial dysfunction and disruption. After the treatment, red fluorescence emitted by JC1 vital mitochondria was found decreased with respect to the control indicating that mitochondrial function had been inhibited (Fig. 7 A and C). Then, synaptosomes were administered in different dose and re-observed by fluorescence measurements. A dose-dependent increased red fluorescence was observed, indicating that the healthy mitochondria transported by synaptosomes had restored the damaged mitochondrial activity (Fig. 7 A and C). The recovery of mitochondrial activity in damaged LAN5 cells after synaptosomes treatment was also confirmed by microscopy fluorescence inspection (Fig. 7 B and D).

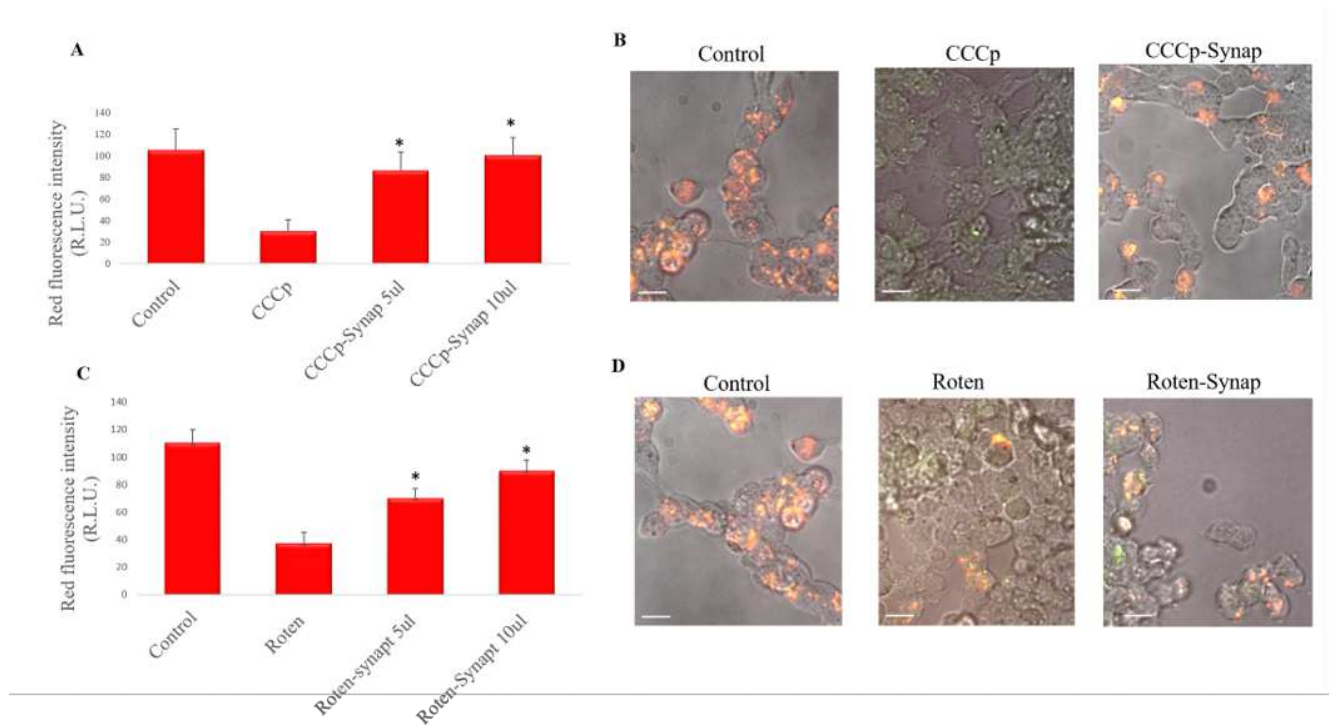


Fig. 7

Discussion

Mitochondrial dysfunction constitutes the base of pathological events including neurological diseases.² Decreasing of ATP production and endogenous antioxidants, increasing of ROS generation and alteration of membrane potential are the main characteristics of damaged mitochondria. Although much work has been done to discover therapeutic drugs targeted to mitochondrial dysfunction, up-to-date no clinical treatment is still available. Mitochondrial transplantation is an innovative technique based on the possibility to replace damaged mitochondria with healthy exogenous mitochondria [16-18]. The most difficult step in the technique is the mitochondria delivery, since during their transfer mitochondria must survive to the transition from an intracellular to an extracellular environment and overcome cell membrane and barriers. Currently applied methodologies for mitochondrial transfer employs naked mitochondria and up to now, no delivery system has been reported. The use of naked mitochondria presents a limit in terms of delivery efficiency, due to the possible occurrence of mitochondrial damage and functional alteration during the isolation and transfer processes associated with no specific cellular target [28-29]. The possibility to encapsulate mitochondria within liposomes has been explored, but some difficulties have been found in organelle packaging [19]. To overcome this problem, it has been recently proposed to use a cell penetrating peptide (Pep-1) conjugated with mitochondria, and improved uptake by the recipient cells and rescue of mitochondrial function were actually observed [20]. Here, we take evidence that synaptosomes can be a neuronal delivery system of naturally encapsulated mitochondria.

Synaptosomes preparation was validated by the presence of Synaptophysin and PSD95 and, consistently with other reports, by intact particles ranging between 0.5-1.5 μm [30]. Further, the high value of the ζ potential and the polydispersity index signified that synaptosomes have good stability, do not tend to flocculate or aggregate and maintain their functional integrity, suggesting that they could be suitable vehicles for the delivery of their cargo, including mitochondria.

An effective delivery system requires an efficient uptake and release of the encapsulate molecules into cells. Nile red or CTX-FITC labelled synaptosomes were internalized into LAN5 recipient cells, as demonstrated by the fluorescence increase and presence of rat synaptophysin. Cellular uptake suggests that synaptosomes can be fused with plasma membrane through a mechanism that appears mediated by specific proteins. After trypsin treatment, indeed, synaptosomes lost their fusion ability. Furthermore, the presence of proteins involved in membrane fusion machinery such as SNARE and SNAP-25 has been demonstrated by synaptosomal proteomic approach. [31]. The specificity of uptake by neuron cells suggests that synaptosomes could contains proteins that act as specific and natural directing agents for

the brain. A similar behaviour has been noticed in exosomes released from stimulated cortical neurons that interact selectively with neurons [32]. In addition, the release ability was demonstrated by presence in LAN5 cellular body of curcumin previously loaded on synaptosomes. Thus, the physical chemical characteristics, the ability of cell uptake, the cargo release and the specific cell targeting, make synaptosomes a natural neuronal delivery system.

The synaptosomes preparation contains mitochondria as demonstrated by the presence of specific mitochondrial proteins such as Opa1, Fis1 and TOM40, and their vitality was confirmed by maintaining of the membrane potential. Furthermore, vital JC1-labeled mitochondria after internalization were released by synaptosomes into the cytosol of neuronal cells as demonstrated by increase of fluorescence. Further, increase of TOM 40, cytochrome C, Hexochinase II proteins and presence of mitochondrial rat DNA, suggests that synaptosomes could be a vehicle for vital mitochondrial transfer. In addition, supplement of healthy mitochondria into cells treated with rotenone or CCCp damaged mitochondria was beneficial to restore the mitochondrial function. Hence, synaptosomes can be both the source and the delivery system of mitochondria.

In physiological condition, mitochondria can be transferred from a donor cell to an injured recipient cell by different contact modes including tunnelling nanotubes, extracellular vesicles, cell-cell fusion, GAP junctions [33-35]. On the basis of these knowledge, McCully and colleagues employed mitochondrial transplantation as therapeutic approach to treat ischemia both in animal models and in pediatric patients [18, 36]. Mitochondrial transplantation is reported as a “magical” cure [28], since healthy organelles, harvested by unaffected tissue, after injection in the ischemic hearth move to the injured cells, rescue ATP energy production and improve the contractile function in 10 minutes [36]. However, this approach, as stated before, present some problems regarding mitochondrial survival during the transfer. Only a little percentage (10%) of the injected mitochondria reaches the target cells and exerts therapeutic effect [17]. Although mitochondrial supplementation has been mainly utilized for cardiac injuries, this approach has been also applied for treatment of neurodegenerative disease and other injuries of the nervous system. [19, 29, 37]. In brain, use of synaptosomes could improve the mitochondrial delivery by protecting the organelle during the transfer, facilitating their specific cellular uptake and reducing stress in the recipient cells. Further, the time of mitochondria transfer could be reduced. The possibility to use synaptosomes as delivery system for mitochondria agrees with the suggested possibility to encapsulate isolated mitochondria in biomaterials for improving their delivery to the brain and subsequent uptake by cells [37]. In addition, to load antioxidant molecules, such as curcumin, within synaptosomes could be an

additional strategy to protect mitochondria by stress occurring during their transfer and/or into the beneficiary cells.

McCully and colleagues indicated that for successful mitochondrial transplantation vital mitochondria once isolated must be immediately used since, as for their experience, frozen mitochondria do not play their cardio protection role [36].

Our findings demonstrate that synaptosomes can be cryopreserved for long time. Indeed, they maintain after thawing their physical-chemical properties and deliver mitochondria vital and physiologically active. Cryopreservation can be a valid strategy in experimental procedures for reducing the number of sacrificed animals and allowing to do experiments whenever required.

Nowadays, brain donation program is one of most valued contribution to scientific research. Differently from other organ donations, brain is not used to be transplanted, but half tissue is used for clinic analyses and half is kept, for eventual scientific studies, in a brain bank. Thus, we cannot exclude that in the future synaptosomes could be extracted from brain of donors, kept in a synaptosomal-bank and used as a source of mitochondria when necessary for transplantation in mitochondria-damaged neuronal cells (Fig. 8).

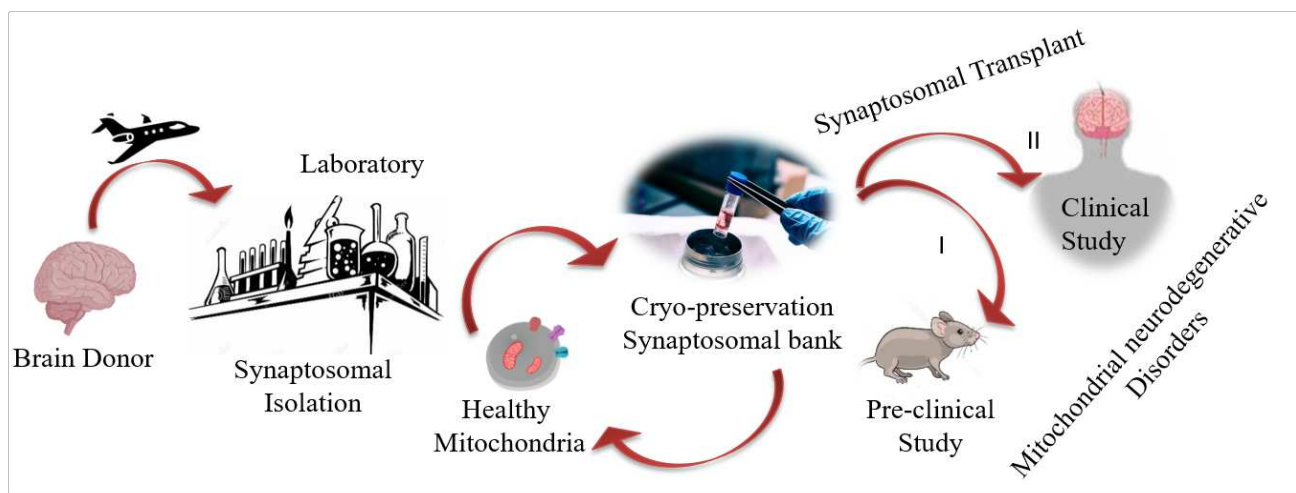


Fig. 8

This procedure could permit to have an always-available source of functional mitochondria ready to be transplanted, overcoming the necessity to isolate fresh mitochondria and reducing the time before transplantation. In medical practice, indeed, it is necessary to obtain functional mitochondria in a short time because protracting surgeries could be counterproductive. However, for clinical application the

criteria of Good Manufacturing Practice (GMP) have to be established. Quality control of size, number, viability and function both of synaptosomes and organelles must be validated. Furthermore, delivery protocols require to be developed for establishing the number of mitochondria-delivered synaptosomes and the administration route. For cardiac injuries, isolated mitochondria have been transplanted by systemic or in situ injection and both the methods have desirable and undesirable effects.²⁹ A high number of mitochondria can be transplanted by systemic injection, but they might be also spread in non-injured tissues [31]. By in situ injection all the isolated mitochondria can be delivered to the target tissue but side effects due to accumulation of the organelles could occur [38]. Further, the injection could not be repeated if necessary during the surgery. In situ transplantation of mitochondria into CNS has been performed in preclinical studies, but its application in clinic results remains arduous [19]. Recently, the possibility to transplant isolated mitochondria in damaged brain through the cerebrospinal fluid (CSF) has been explored [39]. Thus, intraspinal injection could be a new route for transferring mitochondria to the brain and synaptosomes could facilitate the delivery.

Conclusions

Synaptosomes are not only a source of mitochondria, but also a natural delivery system that could improve their neuronal transfer and cellular uptake. Mitochondrial transplantation is a smart strategy to replace or supplement damaged mitochondria. Overall, synaptosomes-mediated mitochondrial transplantation could be applicable for the treatment of many brain diseases in which traditional therapies have demonstrated unsuccessful.

Methods

Synaptosomes isolation from fresh brain tissue

Synaptosomes were isolated by a modification of the method by Franklin et al., (2016) [40]. Briefly, Wistar rats, were purchased from Charles River Laboratories (Calco-Lecco, Italy). Explanted rat brains were donated from Palermo University (Italy) in accordance with the authorization number 69636.N.JCO approved by Italian Ministry of Health (Rome, Italy). The cortex (60 mg) was quickly removed and homogenized in 180 μ L of 0.32M sucrose with 10% protease (Amersham Biosciences, Milan, Italy) and phosphatase cocktail inhibitors (cocktail II and III; Sigma-Aldrich, Milan, Italy) with a Dounce on ice. An aliquot (10 μ l) was immediately flash-freeze in liquid nitrogen and saved as homogenate.

The homogenate (170 μ l) was mixed with 720 μ L of 2M sucrose and 300 μ L of 0.1mM CaCl₂, transferred to 5mL ultracentrifuge tube and ultracentrifuged at 127,000 RCF for 3 hours at 4°C by using TLA110 rotor (Beckman Coulter, Brea, CA). Successively, the myelin layer floating on the top was discarded, and the synaptosomal band at sucrose layers interface was collected (Fig. 1B). Then, the synaptosomal band was transferred into an ultracentrifuge tube and centrifuged at 18,200 RCF for 30 minutes at 4°C in TLA110 rotor (Beckman Coulter, Brea, CA). Supernatant was discarded and the pellet, containing the synaptosomes, was resuspended in 5 mL of HBK buffer (HEPES-buffered Krebs-like) (143 mM NaCl, 4.7 mM KCl, 1.3 mM MgSO₄, 1.2 mM CaCl₂, 20 mM HEPES, 0.1 mM NaH₂PO₄ e 10 mM D-glucose a pH 7.4) to be analysed.

For cryopreservation, the synaptosomal pellet was suspended in 5 mL HBK buffer containing 10% Fetal Bovine Serum (FBS) (Gibco-Invitrogen, Milan, Italy), 10% DMSO, split into 5 aliquots (1mL) and cryopreserved by performing a sequence of controlled freezing steps consisting in 10 minutes at 4°C, overnight at -20 °C, 24-48 hours at -80°C. Finally, the aliquots were stored in liquid nitrogen.

Zeta potential, concentration and polydispersity index

Fresh or thawed Synaptosomal aliquots were resuspended in 2,5ml HBK and diluted (1:100) in PBS 1X. The zeta potential, concentration (particles/ml) and polydispersity index were measured using the instrument ZetaView® BASIC NTA - Nanoparticle Tracking Video Microscope PMX-120.

Quasi-elastic laser light scattering (QELS)

Fresh or thawed Synaptosomal aliquots were resuspended in 2,5ml of HBK ($5.1 \times 10^9 \pm 0.7 \times 10^9$ particles/ml) and QELS experiments were carried out at T 25°C after synaptosomes dilution (1:10) in

HBK at pH 7.4. The cuvette was placed in the thermostatically controlled cell compartment of a Brookhaven Instrument BI200-SM goniometer equipped with a 15 mW He-Neon Spectra Physics laser tuned at λ 632.8 nm. Temperature was controlled within 0.05°C by a circulating bath. Scattered light intensity at 90°, $I_{90^\circ}(t)$, and its time autocorrelation function, $g_2(t)$, were measured by using a Brookhaven BI-9000 correlator. Autocorrelation functions $g_2(t)$ were analysed using a smoothing constrained regularization method CONTIN [41] to obtain the intensity weighted diameter distribution of synaptosomes.

Atomic Force Microscopy (AFM)

Fresh or thawed synaptosomal aliquots were resuspended in 2,5ml HBK and diluted (1:1000). 50 μ l of the synaptosomes suspension were deposited on freshly cleaved mica, washed after few minutes and dried under mild vacuum. Tapping mode AFM images were acquired in air using a multimode scanning probe microscope driven by a Nanoscope V controller (Digital Instruments, Bruker). Single beam uncoated silicon cantilevers (type SPM Probe Mikromasch) were used. The drive frequency was between 260 and 325kHz; the scan rate was 0.25–0.7Hz.

Cell cultures and treatments

LAN5 neuroblastoma, HepG2 human liver cancer and A549 adenocarcinomic human alveolar basal epithelial cell lines, were cultured with RPMI 1640 medium (Celbio srl, Milan, Italy) supplemented with 10% FBS (Gibco-Invitrogen, Milan, Italy), 2 mM glutamine and 1% penicillin, 1% streptomycin (50 mg/mL) (Sigma). The cells were treated with synaptosomes (5.1×10^9 particles/ml), at different dilutions 5-10-20 μ l in 100 μ l of cell medium for 2, 4 or 24 hours.

In transplantation experiments, cells were pre-treated with 40 μ M rotenone for 1 hour and 50 μ M of Carbonyl cyanide 3- chlorophenylhydrazone (CCCp) for 5 minutes at 37°C. After washing, cells were incubated without or with synaptosomes at different dilutions (5-10 μ l in 100 μ l of medium) for 24 hours at 37°C. When indicated, synaptosomes were treated with 1X trypsin (Sigma) or with 50 mM CCCp for 5 min.

Synaptosomes labelling with membrane fluorescence dyes

Fresh or thawed synaptosomal aliquots were resuspended in 2,5ml HBK. 500 μ l of the synaptosomes solution were stained by the membrane dye Nile Red or fluorescein-tagged cholera toxin (CTX-FITC). Nile Red is used to stain lipids since it is highly fluorescent in non-polar environment

(excitation/emission maxima ~535/590). CTx-FITC stains lipid rafts, (excitation/emission maxima 490/535). For staining, synaptosomes were incubated in HBK buffer with Nile Red (5µg/mL) for 15 minutes and with CTX-FITC (10µg/mL) for 30 min at 37 °C in the dark. After incubation, synaptosomes were centrifuged at 10,000 RCF for 10 minutes and then washed two times with HBK to remove the dye excess. Fluorescence emission of synaptosomes marked with Nile Red or CTx-FITC was measured by fluorimeter (Glomax) and fluorescence microscopy (Zeiss).

Cellular uptake of Synaptosomes

For uptake studies, LAN5, HepG2, and A549 cells were plated at the concentration of 3×10^5 cell/mL in 96-well plate. The cells were incubated with different doses (5, 10 and 20µl) of synaptosomes (5.1×10^9 particles/ml), labeled with Nile Red or CTx-FITC for 4 hours. After washing with PBS, the incorporated fluorescence was measured by fluorescence microscope, (Axio Scope 2 microscope; Zeiss) or fluorimeter (Glomax). To compare the fluorescence intensity between the different cell lines, the levels of fluorescence for cell was analysed by Image J software.

Synaptosomes release assay

To test the ability of synaptosomes to release molecules into cells we used curcumin, a natural fluorescent compound. Fresh or thawed synaptosomal aliquots were resuspended in 2,5ml of HBK and curcumin loading was performed by incubating 500µl of synaptosomes with curcumin (5µM) overnight at room temperature. Then, the excess of curcumin in the sample was removed by centrifugation at 10,000 RCF for 10 minutes and two washes with HBK. The amount of curcumin incorporated in synaptosomes was measured by using fluorimeter (Glomax) and fluorescence microscopy (Zeiss). LAN5 cells were plated at the concentration of 3×10^5 cell/mL in a 96-well plate and incubated with 10 or 20µl curcumin-loaded synaptosomes for 2 and 4 hours. After treatment, cells were washed with PBS, and the emitted fluorescence was evaluated by fluorescence microscope, (Axio Scope 2 microscope; Zeiss) or fluorimeter (Glomax) Excitation/emission maxima ~490/535.

Analysis of mitochondrial activity in synaptosomes

Membrane potential of synaptosomal mitochondria was measured using MitoProbe JC-1 assay kit (Thermo Fisher Scientific-US). JC-1 (5,50,6,60-tetrachloro- 1,10,3,30-tetraethylbenzimidazolyl-carbocyanine iodide) is a dye that enters into mitochondria and changes colour from green to red as the membrane potential increases. Fresh or thawed synaptosomal aliquots were resuspended in 2,5ml of

HBK and 100µl were plated in a 96-well plate. After addition of JC-1 (2µM), the sample was incubated for 30 min at 37 °C. CCCp (50 µM), a mitochondrial membrane potential disrupter, was used as control. The excitation length for JC-1 is 490nm, and red and green emission length are 590 and 529 nm, respectively.

Synaptosomal Mitochondria delivery

Fresh or thawed synaptosomal aliquots were resuspended in 2,5ml of HBK and 500µl were incubated with 2µM JC-1 (Thermo Fisher Scientific–US) for 30 min at 37 °C in the dark, and then washed two times in PBS to remove the dye excess. LAN5 cells were plated at the concentrations of 3×10^5 cell/mL in a 96-well plate and incubated with synaptosomes containing with JC-1 marked mitochondria for 2 and 4 hours. After the treatment, cells were washed with PBS, and the fluorescence was evaluated by fluorescence microscope, (Axio Scope 2 microscope; Zeiss). The excitation and emission length were 490 and 590 nm, respectively. The levels of fluorescence for cell was analysed by Image J software.

Total protein extraction and Western blotting

Total proteins were extracted by dissolving cells and synaptosomes in solubilizing buffer (50 mM Tris-HCl pH 7.4, 150 mM NaCl, 0.5% Triton X-100, 2 mM phenylmethylsulphonyl fluoride PMSF, 1mM DTT, 0.1% SDS) with protease inhibitor (Amersham Biosciences, Milan, Italy) and phosphatase inhibitor (cocktail II and III; Sigma Aldrich, Milan, Italy). Protein samples (30 µg) were submitted to 10% SDS PAGE and transferred onto nitrocellulose filters. The Western blot was incubated with anti-TOM40 (1:1000; Cell Signaling, Boston, USA), anti-Cytochrome C (1:1000; Cell Signaling, Boston, USA), anti-OPA1 (1:1000; Cell Signaling, Boston, USA), anti-FIS1(1:1000; Cell Signaling, Boston, USA), anti-synaptophysin (1:2000; Cell Signaling, Boston, USA), PSD95(1:1000; Cell Signaling, Boston, USA), anti-βActin (1:1000; SIGMA) antibodies. Primary antibody was detected by the Odyssey scanner (L-Licor) and using secondary antibody labelled with IR 790, (1:10,000; Life Technology) according to the manufacturer's instructions. Band intensities were analysed with ImageJ and expression was adjusted to βActin expression. The protein levels were expressed as intensity relative to control.

Statistical analysis

All experiments were repeated three times, and in each experiment the samples were taken in triplicate. The results are presented as mean ± SD. Statistical evaluation was conducted by ANOVA, for analysis

of significance. Results with a P value $p \leq 0.05$ were considered statistically significant, * $P \leq 0.05$, ** $P \leq 0.01$.

Acknowledgments

The authors wish to thank Mr. Luca Caruana for its helpful technical support.

Authors contributions: P.P. design and conduction of the research, analysis and interpretation of the data and writing of the initial draft of the manuscript; G.P. and C.C.B, conduction of the research and analysis of the data, D.N. and G.G. conduction of the research, P.L.S.B. and D.B. analysis and interpretation of the data and revision of the manuscript, M.D.C. interpretation of the data, drafting and critical revision of the manuscript. All the authors have read and agreed to the final version of the manuscript.

Funding

This research received no external funding.

Availability of data and materials

The datasets used and/or analyzed during the current study are available from the corresponding author on reasonable request.

Competing interests

The authors declare that they have no competing interests.

Ethics approval and consent to participate

Animal care was in accordance with institutional guideline and with the authorization number 69636.N.JCO approved by Italian Ministry of Health (Rome, Italy).

Consent for publication

No applicable

References

1. Vanni S, Colini Baldeschi A, Zattoni M, Legname G. Brain aging: A Janus-faced player between health and neurodegeneration. *Journal of Neuroscience Research*. 2020;98:299-311.
2. Picone P, Nuzzo D, Caruana L, Scafidi V, Di Carlo M. Mitochondrial dysfunction: different routes to Alzheimer's disease therapy. *Oxidative medicine and cellular longevity*. 2014; 2014: 780179.
3. Zhou Z, Austin G L, Young L, Johnson L A, Sun R. Mitochondrial Metabolism in Major Neurological Diseases. *Cells*. 2018;7:229.
4. Elfawy HA, Das B. Crosstalk between mitochondrial dysfunction, oxidative stress, and age related neurodegenerative disease: Etiologies and therapeutic strategies. *Life sciences*. 2019; 218:165–184.
5. Danta CC, Piplani P. The discovery and development of new potential antioxidant agents for the treatment of neurodegenerative diseases. *Expert opinion on drug discovery* 2014;9:1205–1222.
6. Sun AY, Wang Q, Simonyi A, Sun GY. Resveratrol as a therapeutic agent for neurodegenerative diseases. *Molecular neurobiology*. 2010;41:375–383.
7. Levites Y, Weinreb O, Maor G, Youdim MB, Mandel S. Green tea polyphenol (-)-epigallocatechin-3-gallate prevents N-methyl-4-phenyl-1,2,3,6-tetrahydropyridine-induced dopaminergic neurodegeneration. *Journal of neurochemistry*. 2001;78:1073–1082.
8. Picone P, Nuzzo D, Di Carlo M. Ferulic acid: a natural antioxidant against oxidative stress induced by oligomeric A-beta on sea urchin embryo. *The Biological bulletin*. 2013;224:18–28.
9. Sgarbossa A, Giacomazza D, di Carlo M. Ferulic Acid: A Hope for Alzheimer's Disease Therapy from Plants. *Nutrients*. 2015;7:5764–5782.
10. Picone P, Bondi ML, Montana G, Bruno A, Pitarresi G, Giammona G, Di Carlo, M. Ferulic acid inhibits oxidative stress and cell death induced by Ab oligomers: improved delivery by solid lipid nanoparticles. *Free radical research*. 2009;43:1133–1145.
11. Bondi ML, Montana G, Craparo EF, Picone P, Capuano G, Carlo MD, Giammona G. Ferulic Acid-Loaded Lipid Nanostructures as Drug Delivery Systems for Alzheimer's Disease: Preparation, Characterization and Cytotoxicity Studies. *Current Nanoscience*. 2009;5:26-32.

12. Di Carlo, M., Picone, P., Carrotta, R., Giacomazza, D., & San Biagio, P. L. (2010). Insulin promotes survival of amyloid-beta oligomers neuroblastoma damaged cells via caspase 9 inhibition and Hsp70 upregulation. *Journal of biomedicine & biotechnology*. 2010, 147835.
13. Picone P, Giacomazza D, Vetri V, Carrotta R, Militello V, San Biagio PL, Di Carlo M. Insulin-activated Akt rescues A β oxidative stress-induced cell death by orchestrating molecular trafficking. *Aging cell*. 2011;10:832–843.
14. Picone P, Ditta LA, Sabatino MA, Militello V, San Biagio PL, Di Giacinto ML, Cristaldi L, Nuzzo D, Dispenza C, Giacomazza D, Di Carlo M. Ionizing radiation-engineered nanogels as insulin nanocarriers for the development of a new strategy for the treatment of Alzheimer's disease. *Biomaterials*. 2016;80:179–194.
15. Mishra P, Chan DC. Metabolic regulation of mitochondrial dynamics. *The Journal of cell biology*. 2016;212:379–387.
16. Elliott R, Jiang X, Head J. Mitochondria organelle transplantation: a potential cellular biotherapy for cancer. *J Surgery*. 2015;9:1-3
17. Emani SM, Piekarski BL, Harrild D, Del Nido PJ, McCully JD. Autologous mitochondrial transplantation for dysfunction after ischemia-reperfusion injury. *The Journal of thoracic and cardiovascular surgery*. 2017;154:286–289.
18. McCully JD, Levitsky S, Del Nido PJ, Cowan DB. Mitochondrial transplantation for therapeutic use. *Clinical and translational medicine*. 2016;5:6.
19. Gollihue JL, Patel SP, Rabchevsky AG. Mitochondrial transplantation strategies as potential therapeutics for central nervous system trauma. *Neural regeneration research*. 2018;13:194–197.
20. Chang JC, Hoel F, Liu KH, Wei YH, Cheng FC, Kuo SJ, Tronstad K J, Liu CS.. Peptide-mediated delivery of donor mitochondria improves mitochondrial function and cell viability in human cybrid cells with the MELAS A3243G mutation. *Scientific reports*. 2017;7:10710.
21. Whittaker VP, Michaelson IA, Kirkland RJ. The separation of synaptic vesicles from nerve-ending particles ('synaptosomes'). *The Biochemical journal*. 1964;90:293–303.
22. Jhou JF, Tai HC. The Study of Postmortem Human Synaptosomes for Understanding Alzheimer's Disease and Other Neurological Disorders: A Review. *Neurology and therapy* 2017;6:57–68.
23. Zhang P, Liu G, Chen X. Nanobiotechnology: Cell Membrane-Based Delivery Systems. *Nano today*. 2017;13:7–9.
24. Chu D, Dong X, Shi X, Zhang C, Wang Z. Neutrophil-Based Drug Delivery Systems. *Advanced materials*. 2018;30:e1706245.

25. Igbavboa U, Eckert GP, Malo T M, Studniski AE, Johnson LN, Yamamoto N, Kobayashi M, Fujita SC, Appel TR, Müller WE, Wood WG, Yanagisawa K. Murine synaptosomal lipid raft protein and lipid composition are altered by expression of human apoE 3 and 4 and by increasing age. *Journal of the neurological sciences*. 2005;229-230:225–232.
26. Kadota T, Fujita M, Kadota K. Immunocytochemical localization of synaptophysin on the smooth-surfaced tubular membranes present in nerve terminal and preterminal areas in the rat cerebellar cortex. *Archives of histology and cytology*. 1991;54:519–525.
27. Bondi ML, Craparo EF, Picone P, Di Carlo M, Di Gesu R, Capuano G, Giammona G. Curcumin Entrapped Into Lipid Nanosystems Inhibits Neuroblastoma Cancer Cell Growth and Activates Hsp70 Protein. *Current Nanoscience*. 2010;6:439-445.
28. Bertero E, Maack C, O'Rourke B. Mitochondrial transplantation in humans: "magical" cure or cause for concern? *The Journal of clinical investigation*. 2018;128:5191–5194.
29. Roushandeh AM, Kuwahara Y, Roudkenar MH. Mitochondrial transplantation as a potential and novel master key for treatment of various incurable diseases. *Cytotechnology*. 2019;71:647–663.
30. Postupna NO, Keene CD, Latimer C, Sherfield EE, Van Gelder RD, Ojemann JG, Montine TJ, Darvas M. Flow cytometry analysis of synaptosomes from post-mortem human brain reveals changes specific to Lewy body and Alzheimer's disease. *Laboratory investigation; a journal of technical methods and pathology*. 2014;94:1161–1172.
31. Bai F, Witzmann FA. Synaptosome proteomics. *Sub-cellular biochemistry*. 2007;43:77–98.
32. Chivet M, Javalet C, Laulagnier K, Blot B, Hemming FJ, Sadoul R. Exosomes secreted by cortical neurons upon glutamatergic synapse activation specifically interact with neurons. *Journal of extracellular vesicles*. 2014;3:24722.
33. Murray L, Krasnodembskaya AD. Concise Review: Intercellular Communication Via Organelle Transfer in the Biology and Therapeutic Applications of Stem Cells. *Stem cells*. 2019;37:14–25.
34. Wang J, Li H, Yao Y, Zhao T, Chen YY, Shen Y L, Wang LL, Zhu Y. Stem cell-derived mitochondria transplantation: a novel strategy and the challenges for the treatment of tissue injury. *Stem cell research & therapy*. 2018;9:106.
35. Hough KP, Trevor JL, Strenkowski JG, Wang Y, Chacko BK, Tousif S, Chanda D, Steele C, Antony VB, Dokland T, Ouyang X, Zhang J, Duncan SR, Thannickal VJ, Darley-Usmar VM, Deshane JS. Exosomal transfer of mitochondria from airway myeloid-derived regulatory cells to T cells. *Redox biology*. 2018;18:54–64.

36. Masuzawa A, Black KM, Pacak CA, Ericsson M, Barnett RJ, Drumm C, Seth P, Bloch DB, Levitsky S, Cowan DB, McCully JD. Transplantation of autologously derived mitochondria protects the heart from ischemia-reperfusion injury. *American journal of physiology. Heart and circulatory physiology*. 2013;304:H966–H982.
37. Chang CY, Liang MZ, Chen L. Current progress of mitochondrial transplantation that promotes neuronal regeneration. *Translational neurodegeneration*. 2019;8:17.
38. Shin B, Cowan DB, Emani SM, Del Nido PJ, McCully JD.. Mitochondrial Transplantation in Myocardial Ischemia and Reperfusion Injury. *Advances in experimental medicine and biology*. 2017;982:595–619.
39. Chou SH, Lan J, Esposito E, Ning M, Balaj L, Ji X, Lo E.H, Hayakawa K. (Extracellular mitochondria in cerebrospinal fluid and neurological recovery after subarachnoid hemorrhage. *Stroke*. 2017;48:2231–2237.
40. Franklin W, Tagliatela G. A method to determine insulin responsiveness in synaptosomes isolated from frozen brain tissue. *Journal of neuroscience methods*. 2016;261:128–134.
41. Provencher SW. CONTIN: A general purpose constrained regularization program for inverting noisy linear algebra and integral equations. *Comp.Phys. Commun*. 1982;27:229-242.

Table 1. Concentration (particles/mL), zeta potential and polydispersity index of extracted synaptosomes.

FIG. LEGENDS

Fig. 1. Synaptosomes isolation and characterization. A) Representation of synaptosomal particles with pre- and post-synaptic areas evidenced. B) Synaptosomal band (red arrow) collected at sucrose interface after ultracentrifugation in sucrose fractionation. C) Western blot of proteins extracted from total homogenate (Total) and synaptosomal fraction (Synapt) incubated with anti-PSD95 (PSD95) and anti-Synaptophysin (SyP). D) Relative quantification of the immunoreactive bands. The uniformity of gel loading was confirmed by using β -actin as a standard. * $P < 0.05$, vs total homogenate (Total). E) Intensity weighted size distribution functions of the synaptosomes extracted. F) AFM images of the synaptosomes extracted.

Fig. 2. Synaptosomes can interact with Cells. A) Histogram of fluorescence intensity and fluorescence image of synaptosomes stained with Nile Red (Synap Nile Red) and related cartoon. B) Histogram of fluorescence intensity and fluorescence image of synaptosomes stained with CTX-FITC (Synap CTX-FITC) and related cartoon. C) Cartoon of neuronal cells incubated with synaptosomes stained with Nile Red or CTX-FITC. D) Histogram of fluorescence intensity of LAN5 cells incubated with different doses of synaptosomes labeled with Nile Red (Synap Nile Red 5-10 and 20 μ l). E) Representative fluorescence images of Synap NileRed and LAN5 cells interaction, nuclei stained with Hoechst 33342. F) Fluorescent intensity histogram of LAN5 cells incubated with different doses of synaptosomes labeled with CTX-FITC (Synap CTX-FITC 5-10 and 20 μ l). G) Representative fluorescence images of Synap CTX-FITC and LAN5 cells interaction. Nuclei were stained with Hoechst 33342. H) Schematic representation of the localization of Rat synaptophysin (Rat SyP) (red) and Human synaptophysin (Human SyP) (yellow) before and after administration of synaptosomes in LAN5 cell. I) Western blot analysis of proteins extracted from LAN5 cells untreated (Control) or treated with different doses of synaptosomes (5-10-20 μ l) (Lan5+synap), and from synaptosomes incubated with anti-Synaptophysin (SyP). L) Relative quantification of Rat synaptophysin (Rat SyP) immunoreactive band (36 kDa). The uniformity of gel loading was confirmed by using β -actin as a standard. *P < 0.05, **P < 0.02 vs Control. Scale bar 20 μ m.

Fig. 3. Synaptosomes are able to load and release curcumin. A) Histogram of the fluorescence intensity and fluorescence image of synaptosomes loaded with Curcumin (Synap-Curcumin). B) Schematic representation of LAN5 neuronal cell incubated with Synap-Curcumin. C) Histogram of the fluorescence intensity of LAN5 cells incubated with different doses (10-20 μ l) of Synap-Curcumin for 2 and 4 hours. D) Representative fluorescence images showing the interaction of Synap-Curcumin with LAN5 cells and control (not treated). Nuclei were stained with Hoechst 33342. *P < 0.05, **P < 0.02 vs Control. Scale bar 20 μ m.

Fig. 4 Synaptosomes–cell interaction depends on specific proteins. A) Schematic representation of synaptosomes labeled with Nile Red and incubated with trypsin (Synap-NileRed-Tryp) before incubation with LAN5 cells. B) Histogram of fluorescence intensity for LAN5 cells incubated with Synap-NileRed-Tryp and Synap-NileRed at different doses (10-20 μ l) and for the relative control (untreated cells). C) Representative fluorescence images for LAN5 cells incubated with Synap-NileRed and Synap-NileRed-Tryp. Nuclei were stained with Hoechst 33342. **P < 0.02. D) Representative fluorescence images of

LAN5, A549 and HepG2 cells after incubation with Nile Red labeled Synaptosomes. Nuclei were stained with Hoechst 33342. E) Histogram of the relative fluorescence intensity for the three types of cells. **P < 0.02 vs LAN5. Scale bar 20 μ m.

Fig. 5. Synaptosomes contain vital mitochondria. A) Western blotting analysis of proteins extracted from total homogenate (Total) and synaptosomal fraction (Synapt) incubated with antibodies against the mitochondrial proteins Opa1, Fis1 and TOM40. B) Red and green fluorescence intensity for synaptosomes incubated with or without (Synap) JC1 and for synaptosomes treated with CCCp and incubated with JC-1 (Synap-JC1-CCCp) (positive control). C) Representative JC1 fluorescence images of synaptosomes incubated with or without (Synap-JC1) CCCp. Cryopreservation of Synaptosomes D) Schematic representation of the synaptosomes freezing procedure. E) Table of the values of mean diameter and zeta potential of fresh and thawed synaptosomes. F) Red and green fluorescence intensity of fresh (fresh Synap-JC1) and thawed (thawed Synap-JC1) synaptosomes incubated with JC-1. G) Representative JC1 red fluorescence images of fresh and thawed synaptosomes incubated with JC-1. **P < 0.02 vs Control. Scale bar 20 μ m.

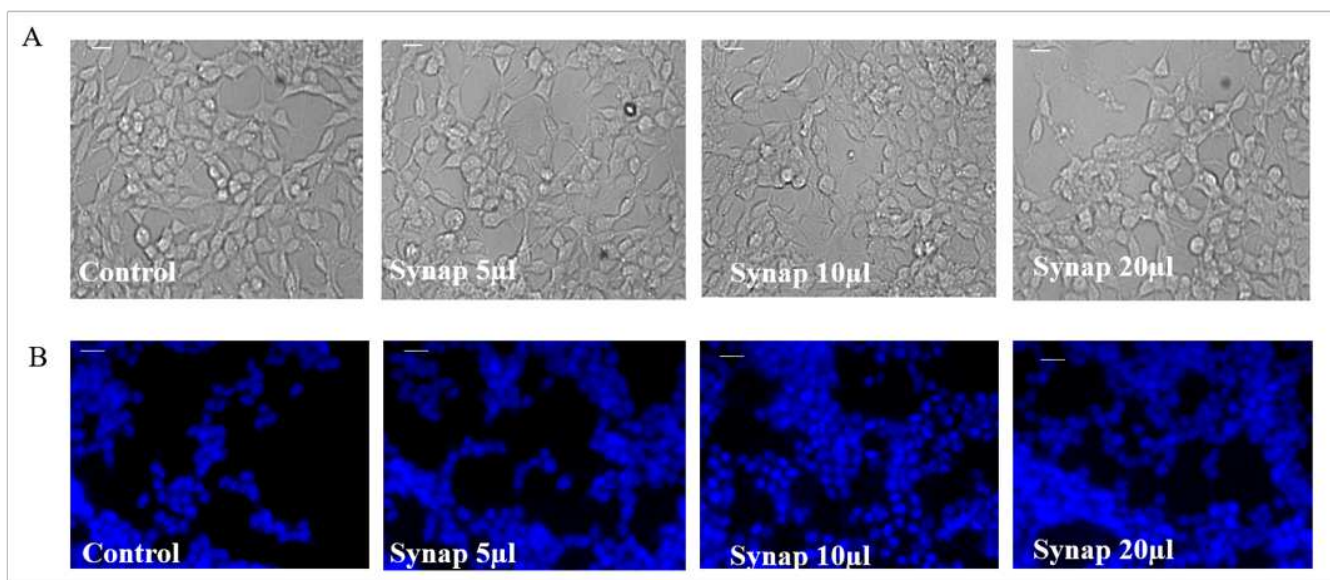
Fig. 6. Synaptosomes can vehicle mitochondria A) Cartoon of synaptosomes containing JC1-stained mitochondria (Synap-JC1) administered to LAN5 neuronal cells. B) Representative bright field and red fluorescence images showing the interaction between Synap-JC1 and LAN5 cells after 2 or 4h of incubation. C) Representative dynamic imaging of Synap-C-1 at different times. D) Histogram of the relative JC1 red fluorescence intensity for cell incubated with Synap-JC1 for 2 and 4 hours. E) Western blot of proteins extracted from LAN5 untreated (Control) or synaptosomes treated (Synap) and incubated with antibodies against mitochondrial proteins TOM40, Cytochrome C (Cyt C) and Hexokinase II (Hexok) F) Relative quantification of the immunoreactive bands. The uniformity of gel loading was confirmed by using β -actin as standard. G) PCR analysis of the mitochondrial DNA (mtDNA) specific for Human (Human mtDNA) and Rat (Rat mtDNA) in human LAN5 cells incubated with rat synaptosomes at different doses (5 and 10 μ l). Human nuclear DNA (Human nDNA) was used as reference. *P < 0.05, **P < 0.02 vs Control. Scale bar 20 μ m.

Fig. 7. Synaptosomes can replace damaged mitochondria. A) Histogram of JC1 red fluorescence intensity for LAN5 cell untreated (Control) or treated with CCCp (CCCp) alone or with synaptosomes (CCCp- Synap) at different doses (5 and 10 μ l). B) Representative images of LAN5 untreated (Control)

or incubated with CCCp alone or with synaptosomes (CCCp- Synap) after JC-1 assay. C) Histogram of JC1 red fluorescence intensity for LAN5 cell untreated (Control) or treated with Rotenone (Roten) alone or with synaptosomes (Roten-synap) at different doses (5 and 10 μ l). D) Representative images of LAN5 untreated (Control) or incubated with Rotenone (Roen) alone or with synaptosomes (Roten- Synap) after JC-1 assay. *P < 0.05, vs CCCp or Rotenon. Scale bar 20 μ m.

Fig. 8. Schematic representation of the step sequence to build a postmortem synaptosomal bank to be used as a reserve of mitochondria for transplantation in pre-clinical and/or clinical studies on neurodegenerative diseases.

SUPPORTING INFORMATION



S1. A) Morphological analysis of LAN5 cells incubated with different doses (5-10 and 20 μ l) of synaptosomes (Synap). B) Nuclear staining by fluorescence probe Hoechst 3341 of LAN5 cells incubated with different doses (5-10 and 20 μ l) of synaptosomes (Synap).

ORCID

Pasquale Picone: <https://orcid.org/0000-0001-7127-2183>

Marta Di Carlo <https://orcid.org/0000-0002-7934-1275>

Figures

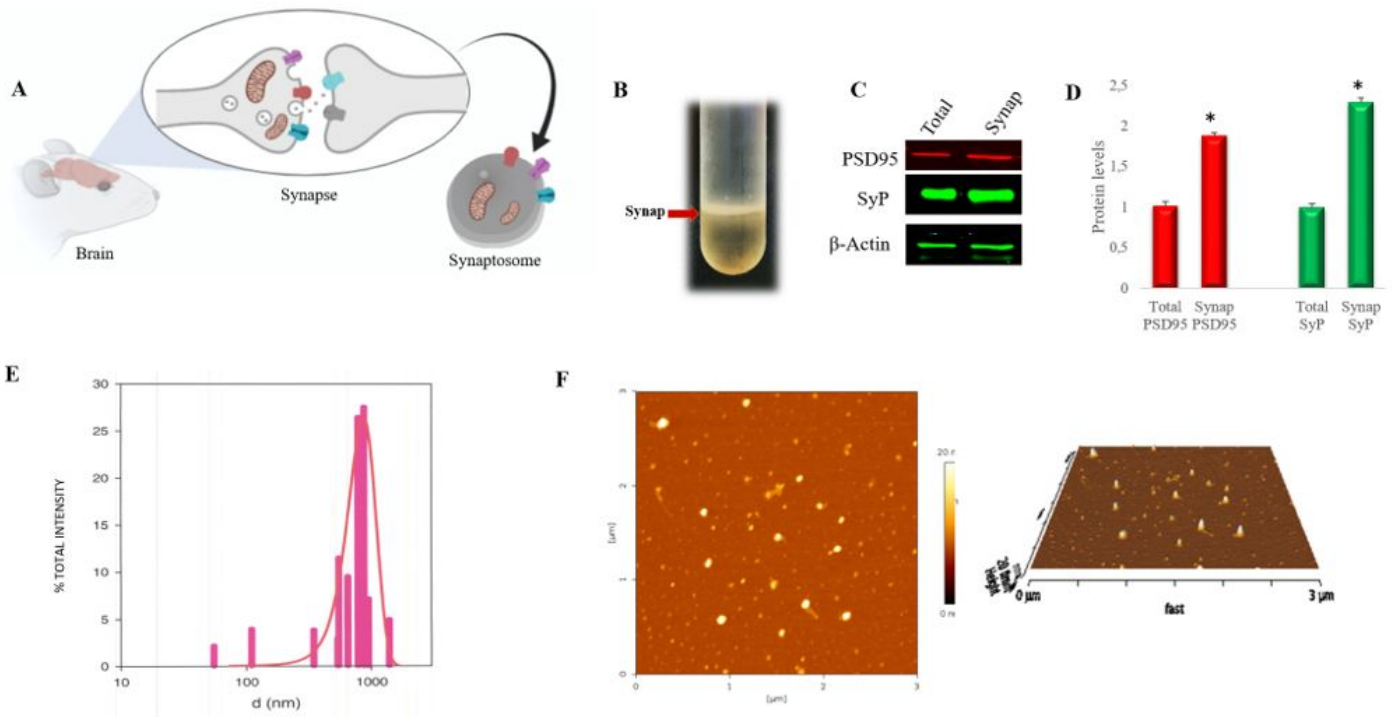


Figure 1

Synaptosomes isolation and characterization. A) Representation of synaptosomal particles with pre- and post-synaptic areas evidenced. B) Synaptosomal band (red arrow) collected at sucrose interface after ultracentrifugation in sucrose fractionation. C) Western blot of proteins extracted from total homogenate (Total) and synaptosomal fraction (Synap) incubated with anti-PSD95 (PSD95) and anti-Synaptophysin (SyP). D) Relative quantification of the immunoreactive bands. The uniformity of gel loading was confirmed by using β -actin as a standard. * $P < 0.05$, vs total homogenate (Total). E) Intensity weighted size distribution functions of the synaptosomes extracted. F) AFM images of the synaptosomes extracted.

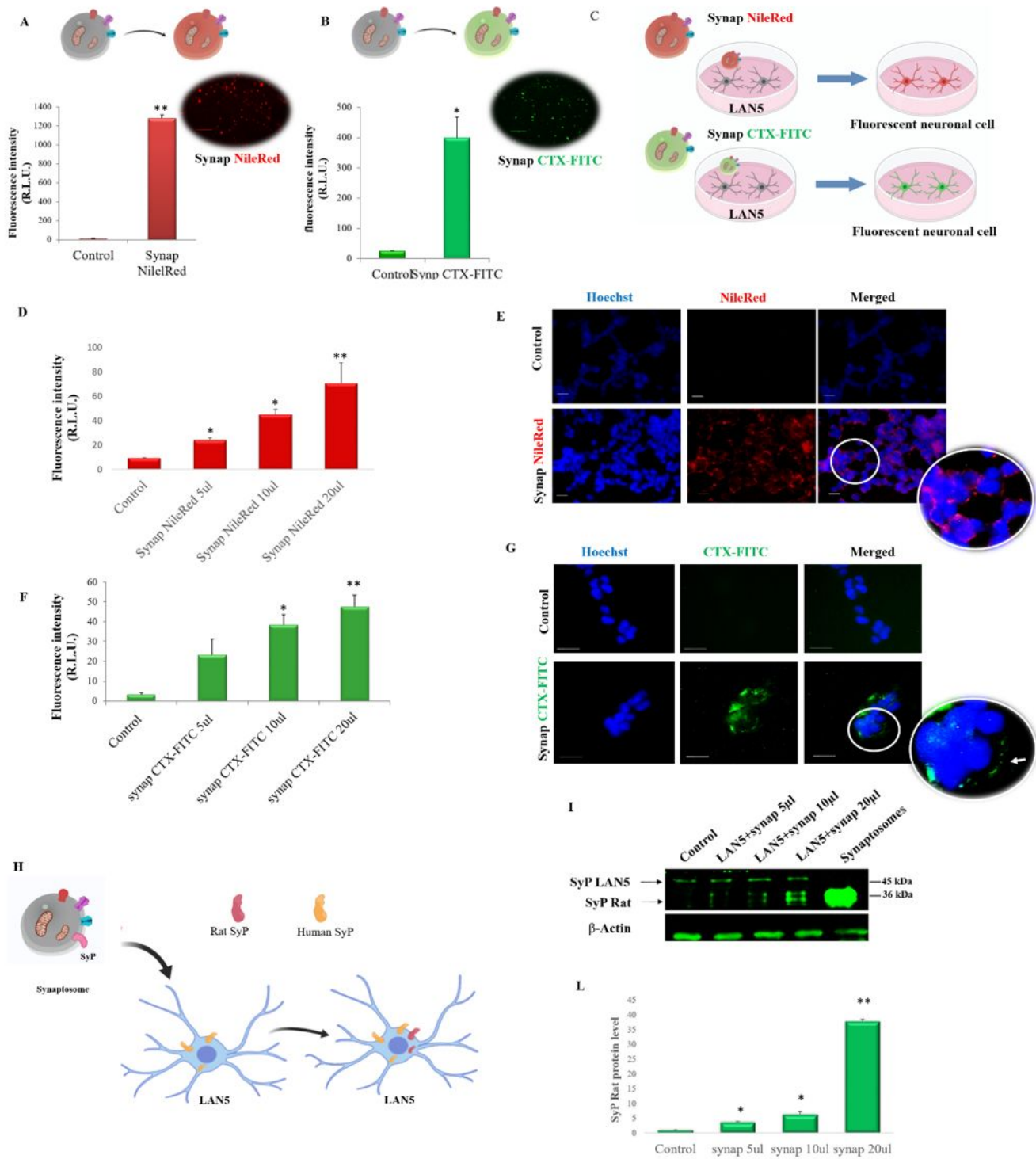


Figure 2

Synaptosomes can interact with Cells. A) Histogram of fluorescence intensity and fluorescence image of synaptosomes stained with Nile Red (Synap Nile Red) and related cartoon. B) Histogram of fluorescence intensity and fluorescence image of synaptosomes stained with CTX-FITC (Synap CTXFITC) and related cartoon. C) Cartoon of neuronal cells incubated with synaptosomes stained with Nile Red or CTX-FITC. D) Histogram of fluorescence intensity of LAN5 cells incubated with different doses of synaptosomes

labeled with Nile Red (Synap Nile Red 5-10 and 20 μ l). E) Representative fluorescence images of Synap NileRed and LAN5 cells interaction, nuclei stained with Hoechst 33342. F) Fluorescent intensity histogram of LAN5 cells incubated with different doses of synaptosomes labeled with CTXFITC (Synap CTX-FITC 5-10 and 20 μ l). G) Representative fluorescence images of Synap CTX-FITC and LAN5 cells interaction. Nuclei were stained with Hoechst 33342. H) Schematic representation of the localization of Rat synaptophysin (Rat SyP) (red) and Human synaptophysin (Human SyP) (yellow) before and after administration of synaptosomes in LAN5 cell. I) Western blot analysis of proteins extracted from LAN5 cells untreated (Control) or treated with different doses of synaptosomes (5-10-20 μ l) (Lan5+synap), and from synaptosomes incubated with anti-Synaptophysin (SyP). L) Relative quantification of Rat synaptophysin (Rat SyP) immunoreactive band (36 kDa). The uniformity of gel loading was confirmed by using β -actin as a standard. *P < 0.05, **P < 0.02 vs Control. Scale bar 20 μ m.

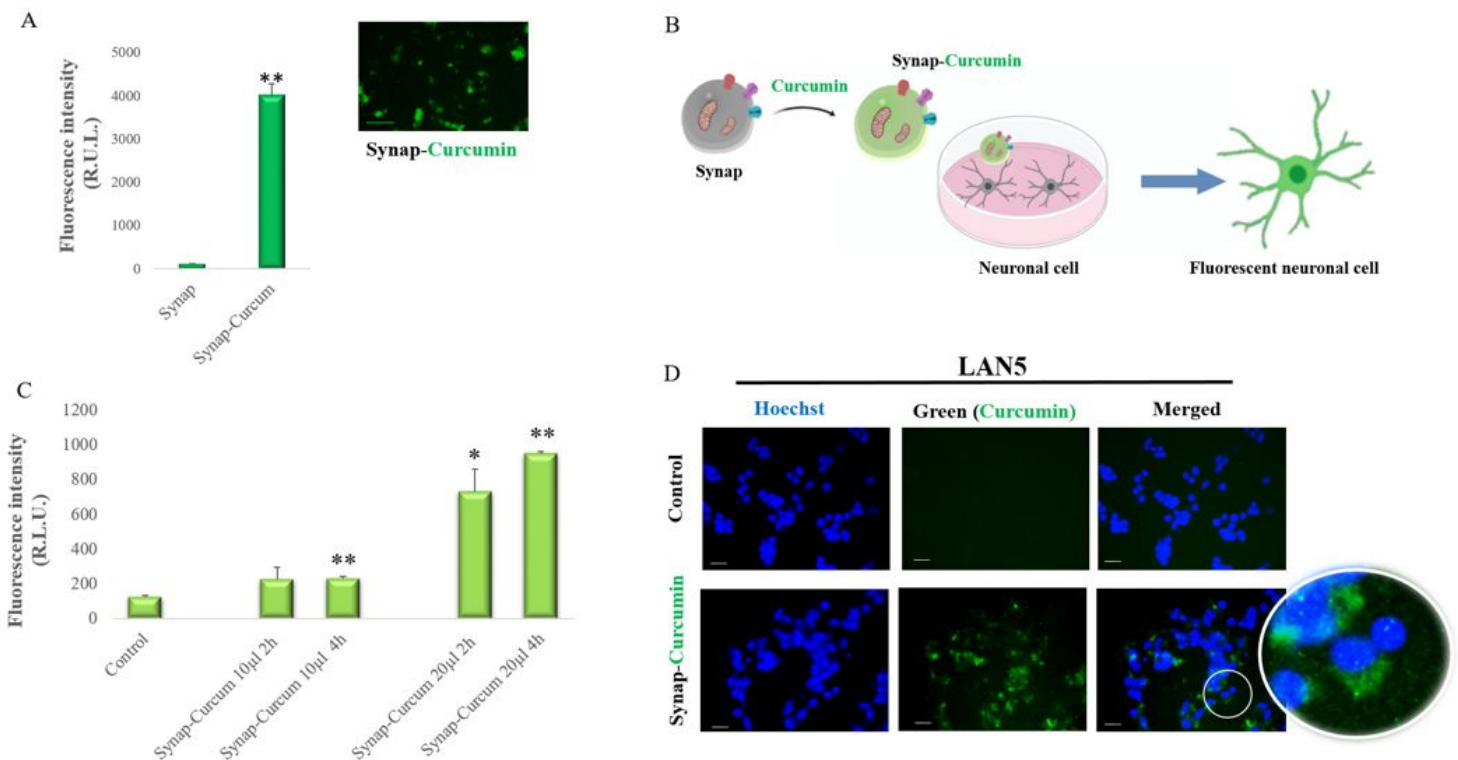


Figure 3

Synaptosomes are able to load and release curcumin. A) Histogram of the fluorescence intensity and fluorescence image of synaptosomes loaded with Curcumin (Synap-Curcumin). B) Schematic representation of LAN5 neuronal cell incubated with Synap-Curcumin. C) Histogram of the fluorescence intensity of LAN5 cells incubated with different doses (10-20 μ l) of Synap-Curcumin for 2 and 4 hours. D) Representative fluorescence images showing the interaction of Synap-Curcumin with LAN5 cells and control (not treated). Nuclei were stained with Hoechst 33342. *P < 0.05, **P < 0.02 vs Control. Scale bar 20 μ m.

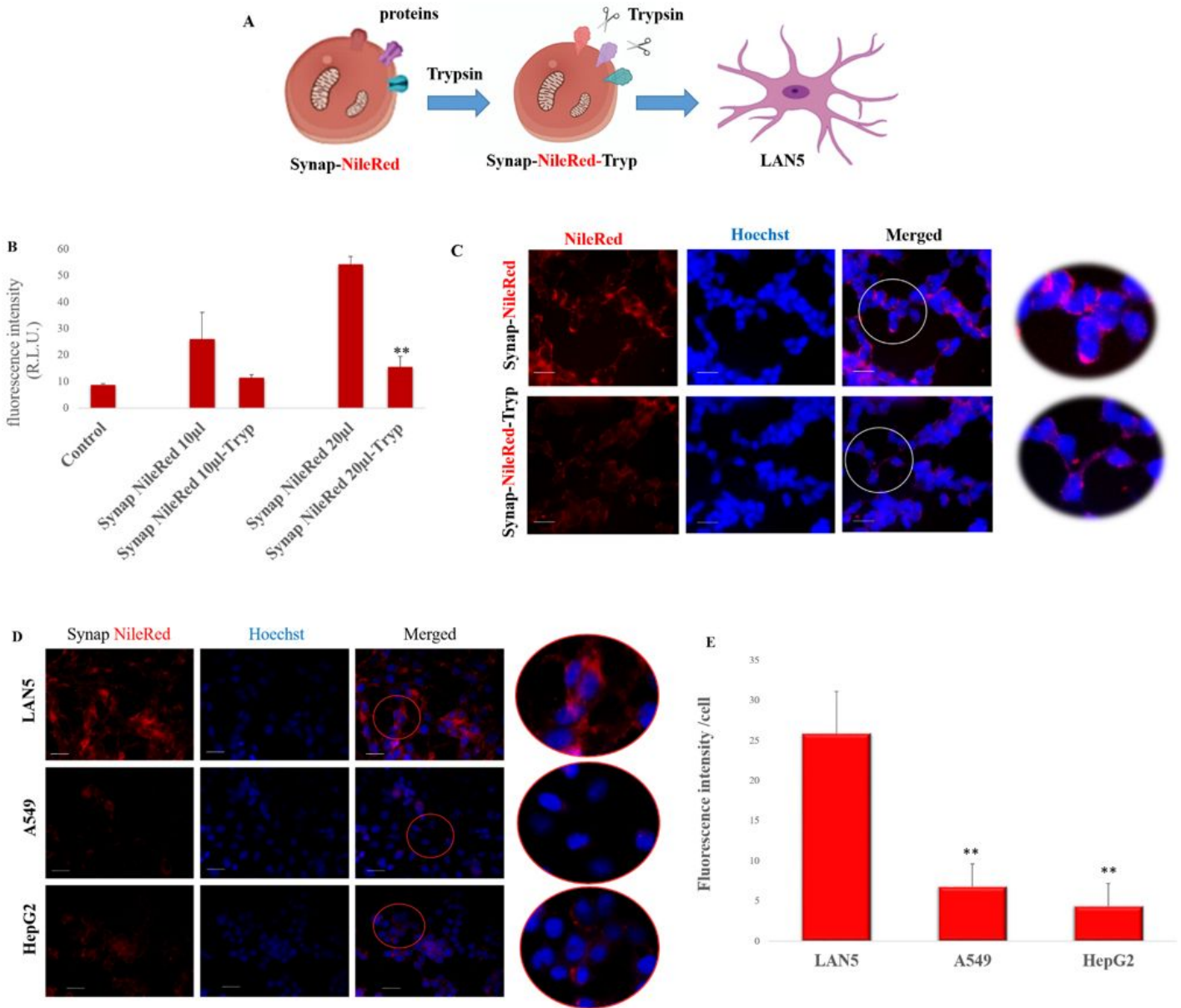


Figure 4

Synaptosomes–cell interaction depends on specific proteins. A) Schematic representation of synaptosomes labeled with Nile Red and incubated with trypsin (Synap-NileRed-Tryp) before incubation with LANS5 cells. B) Histogram of fluorescence intensity for LANS5 cells incubated with Synap-NileRed-Tryp and Synap-NileRed at different doses (10-20 µl) and for the relative control (untreated cells). C) Representative fluorescence images for LANS5 cells incubated with Synap-NileRed and Synap-NileRed-Tryp. Nuclei were stained with Hoechst 33342. **P < 0.02. D) Representative fluorescence images of LANS5, A549 and HepG2 cells after incubation with Nile Red labeled Synaptosomes. Nuclei were stained with Hoechst 33342. E) Histogram of the relative fluorescence intensity for the three types of cells. **P < 0.02 vs LANS5. Scale bar 20µm

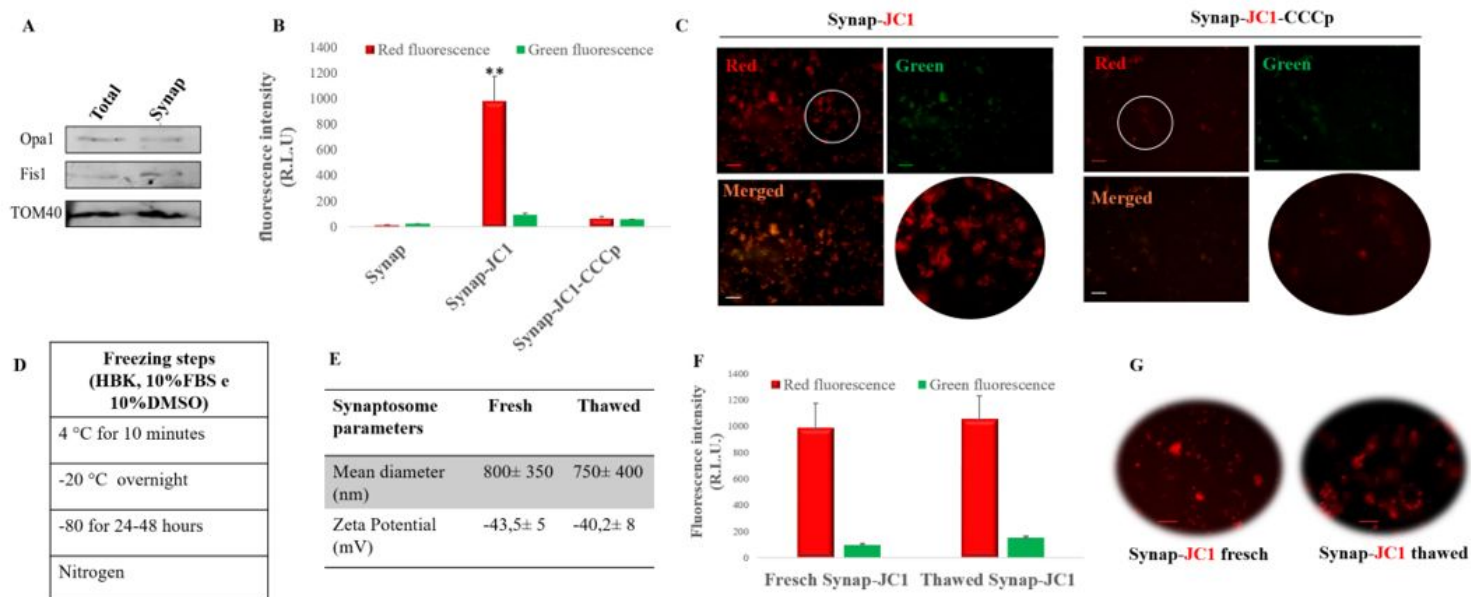


Figure 5

Synaptosomes contain vital mitochondria. A) Western blotting analysis of proteins extracted from total homogenate (Total) and synaptosomal fraction (Synap) incubated with antibodies against the mitochondrial proteins Opa1, Fis1 and TOM40. B) Red and green fluorescence intensity for synaptosomes incubated with or without (Synap) JC1 and for synaptosomes treated with CCCp and incubated with JC-1 (Synap-JC1-CCCp) (positive control). C) Representative JC1 fluorescence images of synaptosomes incubated with or without (Synap-JC1) CCCp. Cryopreservation of Synaptosomes D) Schematic representation of the synaptosomes freezing procedure. E) Table of the values of mean diameter and zeta potential of fresh and thawed synaptosomes. F) Red and green fluorescence intensity of fresh (fresh Synap-JC1) and thawed (thawed Synap-JC1) synaptosomes incubated with JC-1. G) Representative JC1 red fluorescence images of fresh and thawed synaptosomes incubated with JC-1. **P < 0.02 vs Control. Scale bar 20µm.

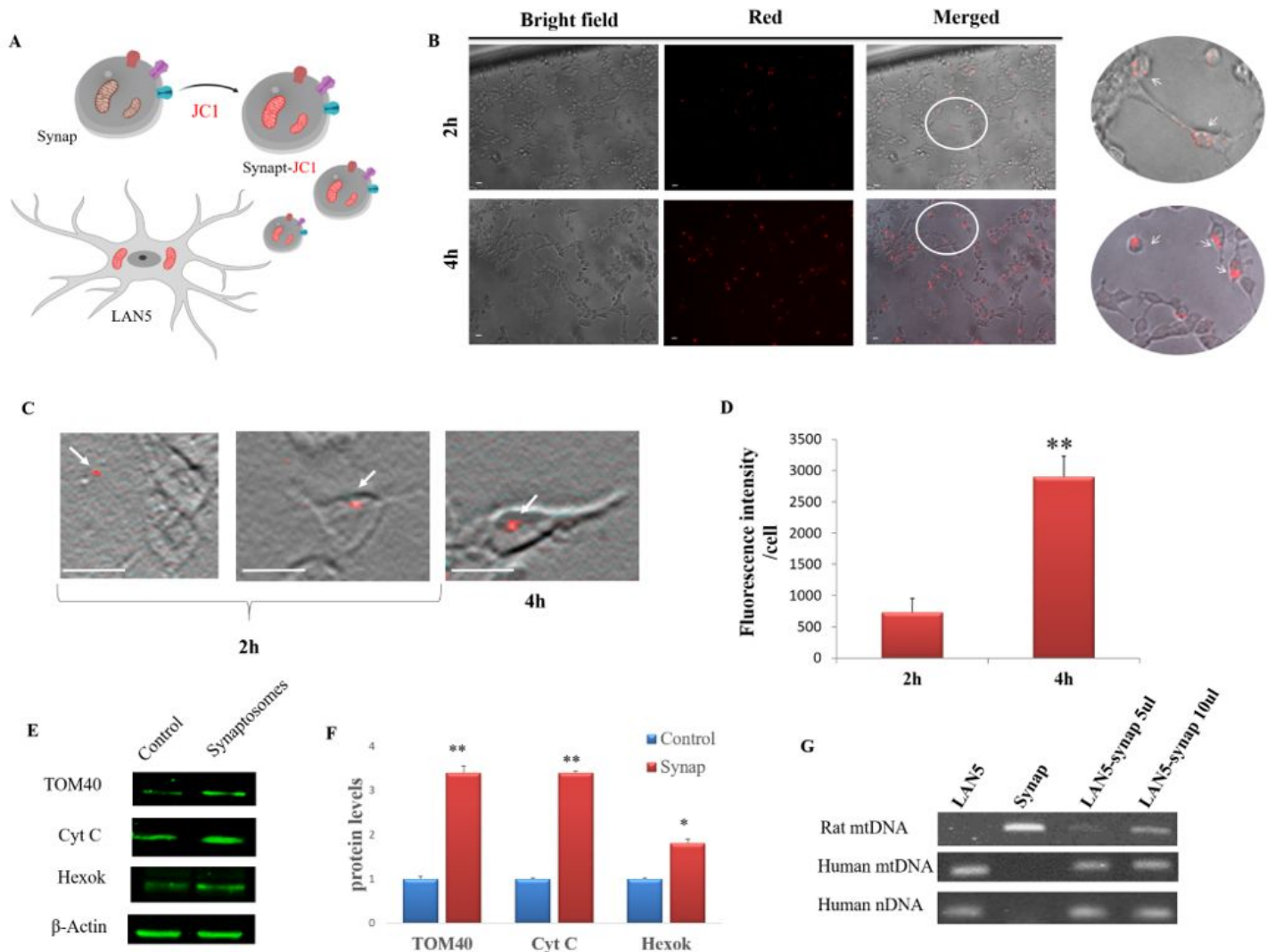


Figure 6

Synaptosomes can vehicle mitochondria A) Cartoon of synaptosomes containing JC1-stained mitochondria (Synap-JC1) administered to LANS5 neuronal cells. B) Representative bright field and red fluorescence images showing the interaction between Synap-JC1 and LANS5 cells after 2 or 4h of incubation. C) Representative dynamic imaging of Synap-JC1 at different times. D) Histogram of the relative JC1 red fluorescence intensity for cell incubated with Synap-JC1 for 2 and 4 hours. E) Western blot of proteins extracted from LANS5 untreated (Control) or synaptosomes treated (Synap) and incubated with antibodies against mitochondrial proteins TOM40, Cytochrome C (Cyt C) and Hexokinase II (Hexok) F) Relative quantification of the immunoreactive bands. The uniformity of gel loading was confirmed by using β -actin as standard. G) PCR analysis of the mitochondrial DNA (mtDNA) specific for Human (Human mtDNA) and Rat (Rat mtDNA) in human LANS5 cells incubated with rat synaptosomes at different doses (5 and 10 μ l). Human nuclear DNA (Human nDNA) was used as reference. *P < 0.05, **P < 0.02 vs Control. Scale bar 20 μ m.

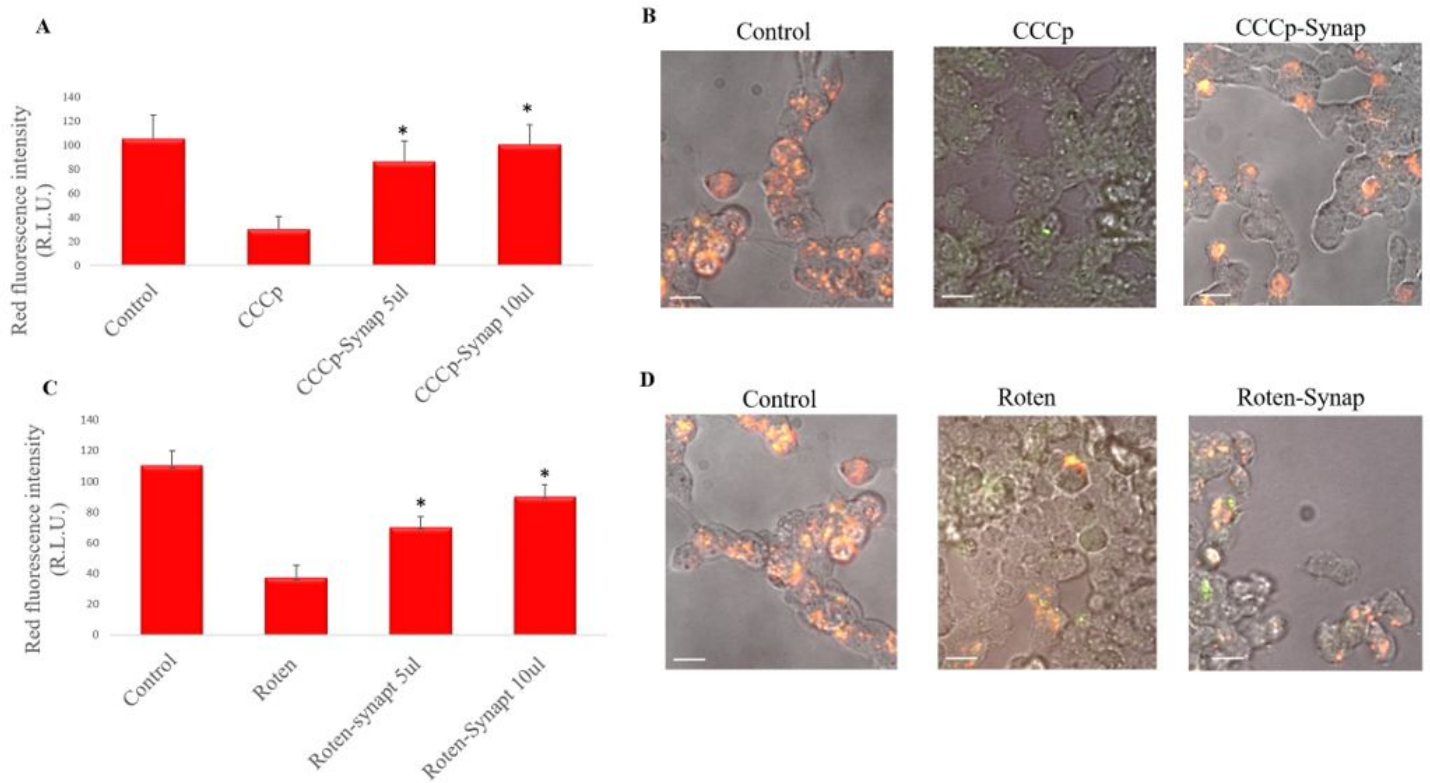


Figure 7

Synaptosomes can replace damaged mitochondria. A) Histogram of JC1 red fluorescence intensity for LAN5 cell untreated (Control) or treated with CCCp (CCCp) alone or with synaptosomes (CCCp- Synap) at different doses (5 and 10 μ l). B) Representative images of LAN5 untreated (Control) or incubated with CCCp alone or with synaptosomes (CCCp- Synap) after JC-1 assay. C) Histogram of JC1 red fluorescence intensity for LAN5 cell untreated (Control) or treated with Rotenone (Roten) alone or with synaptosomes (Roten-synap) at different doses (5 and 10 μ l). D) Representative images of LAN5 untreated (Control) or incubated with Rotenone (Roen) alone or with synaptosomes (Roten- Synap) after JC-1 assay. *P < 0.05, vs CCCp or Rotenon. Scale bar 20 μ m.

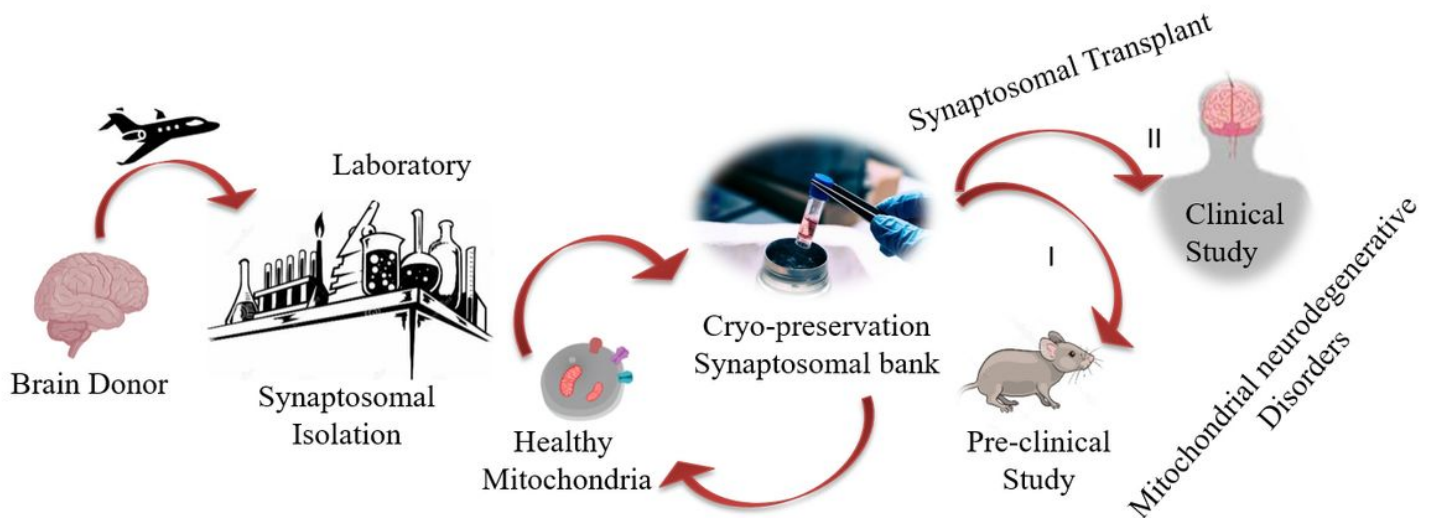


Figure 8

Schematic representation of the step sequence to build a postmortem synaptosomal bank to be used as a reserve of mitochondria for transplantation in pre-clinical and/or clinical studies on neurodegenerative diseases.

Supplementary Files

This is a list of supplementary files associated with this preprint. Click to download.

- [FigS1.JPG](#)